ANTENNA SELECTION AND PERFORMANCE

ANALYSIS OF MIMO SPATIAL MULTIPLEXING

SYSTEMS

Hassan A. Abou Saleh

A Thesis

in

The Department

of

Electrical and Computer Engineering

Presented in Partial Fulfillment of the Requirements

For the Degree of Master of Applied Science

Concordia University

Montréal, Québec, Canada

August 2008

Canada

ABSTRACT

Antenna Selection and Performance Analysis of MIMO Spatial

Multiplexing Systems

Hassan A. Abou Saleh

Multiple-input multiple-output spatial multiplexing (MIMO-SM) systems offer an essential benefit referred to as spatial multiplexing gain. Two important signal reception techniques for MIMO-SM systems are the zero-forcing (ZF) and ordered successive interference cancellation (OSIC) as, for example, in the case of the decision-feedback detector (DFD). This thesis studies the communication and signal processing aspects of MIMO-SM. We first investigate the bit error rate (BER) performance of the ZF receiver over transmit correlated Ricean flat-fading channels. In particular, for a MIMO channel with M transmit and N receive antennas, we derive an approximation for the average BER of each substream. A closed-form expression for the optimal transmit correlation coefficient, which achieves the maximum capacity (i.e., uncorrelated case) of two-input two-output spatial multiplexing (TITO-SM) systems, is presented.

We further propose an antenna selection (AS) approach for the DFD over independent Rayleigh flat-fading channels. The selected transmit antennas are those that maximize both the post-processing signal-to-noise ratio (SNR) at the receiver end, and the system capacity. An upper bound on the outage probability for the AS approach is derived. It is shown that the AS approach achieves a performance comparable to optimal capacity-based selection based on exhaustive search, but at a lower complexity.

Finally, we investigate a cross-layer transmit AS approach for the DFD over spatially correlated Ricean flat-fading channels. The selected transmit antennas are those that maximize the link layer throughput of correlated MIMO channels. A closed-form expression for the system throughput with perfect channel estimation is first derived. We further analyze the system performance with pilot-aided channel estimation. In that, we derive a closed-form expression for the post-detection signal-to-noise-plus-interference ratio (SNIR) of each transmitted substream, conditioned on the estimated channels. The derived SNIR is then used to evaluate the overall system throughput. It is observed that the the cross-layer AS approach always assigns the transmission to the antenna combination which sees better channel conditions, resulting in a substantial improvement over the optimal capacity-based AS approach. Considering a training-based channel estimation technique, we compare the performance of the proposed cross-layer AS with that of optimal capacity-based AS when employed with a training-based channel estimation. Our results show that the latter is more robust to imperfect channel estimation. However, in all cases, the cross-layer AS delivers higher throughput gains than the capacity-based AS.

Acknowledgments

Foremost, I thank my supervisor, Dr. Walaa Hamouda, for his guidance, inspiration, and encouragement in the past two years. Dr. Hamouda provided me the invaluable opportunity to investigate those fascinating research problems and always showed full confidence in me. Without Dr. Hamouda's constructive suggestions and knowledgeable guidance in communication and signal processing area, this work would not have been successfully completed.

I am indebted to my parents and brothers for their continuous encouragements and expectations. I just hope I can live up to their expectations in my future career. Special thanks go to Dr. Iyad Kanj for his encouragement and invaluable advices. I am also grateful to my friends who made the last two years full of fun: Mohanad whose discussions have benefited me a lot; Hamza and Saeed who always stood beside me when I needed help; Khoder, Imad for their company and friendship. I would like also to thank Ariel for providing me with the LaTeX template. Finally, I would like to thank Dr. M. R. Soleymani, and Dr. A. M. Youssef for serving in my thesis committee.

This thesis is dedicated to my parents, brothers, cousins, and my homeland.

Contents

List of Figures

List of Important Symbols

M	number of transmit antennas
N	number of receive antennas
$\mathbf{H}$	channel matrix
$(\cdot)^T$	transpose
$\mathcal{A}$	symbol constellation set
$CN(\cdot)$	complex normal distribution
N_0	noise variance
$\mathbf{I}$	identity matrix
P_x	total average energy over a symbol period (i.e., total input power)
$\mathbb{E}[\cdot]$	expectation
$(\cdot)^H$	conjugate transpose
ζ	input SNR
$\mathcal{M}$	size of the symbol constellation set $\mathcal{A}$
$\|\cdot\|$	Frobenius norm
$(\hat{\cdot})$	data estimate
$\mathbf{G}$	matrix equalizer
C	mapping to the nearest point in the symbol constellation (slicer)
$(\cdot)^\dagger$	Moore-Penrose pseudoinverse
γ_0	average normalized SNR at each receive antenna
δ	Dirac's delta
D	diversity order

C	complex plane
$\mathbf{R}_t$	transmit correlation matrix
$\bar{\mathbf{H}}_{\text{LOS}}$	LOS component
$\bar{\mathbf{H}}_w$	independent and identically distributed Rayleigh component
κ	Ricean factor
$\boldsymbol{\Psi}$	matrix of all ones
$\otimes$	Kronecker product of matrices
$\boldsymbol{\Sigma}$	covariance matrix of $\mathbf{H}$
ρ	transmit correlation coefficient
$(\cdot)^*$	complex conjugate
CW_M	Wishart distribution
$\boldsymbol{\Sigma}'$	approximate covariance matrix
$[\boldsymbol{\Sigma}']^{-1}_{kk}$	(k,k)th element of the matrix $[\boldsymbol{\Sigma}']^{-1}$
$\Gamma(\cdot)$	Gamma function
$\det[\cdot]$	determinant
$Q(\cdot)$	complementary error function
$\mathbf{R}_r$	receive correlation matrix
r_{Rx}	receive correlation coefficient
$\mathbb{C}$	instantaneous capacity
ρ_{opt}	optimal transmit correlation coefficient
K	number of selected transmit antennas
p	optimal subset of transmit antennas
$\mathbf{H}_p$	channel submatrix corresponding to the K selected transmit antennas
$\mathbf{E}_p$	channel-dependent permutation matrix corresponding to the detection ordering of $\mathbf{H}_p$
$\mathbb{R}$	real plane
$\mathbf{Q}$	$N \times M$ semi-unitary matrix with its orthonormal columns being the zero-forcing nulling vectors
$\mathbf{R}$	$M \times M$ upper triangular matrix with real-valued positive diagonal entries

E	channel-dependent permutation matrix corresponding to the detection ordering of **H**
$r_{i,i}$	(i,i)th entry of **R**
Δe_j	error term resulting from the hard/soft estimate made on the x_j symbol
$\mathcal{R}$	information transmission rate
$\mathcal{P}_{\text{outage,AS}}$	outage probability for the AS scheme
$\mathcal{F}_{r_{v,v}^2}(\cdot)$	CDF of the random variable $r_{v,v}^2$
χ^2	chi-squared variate
L	frame length
η	system throughput
W	window size
$\Delta \mathbf{H}_p$	estimation error matrix corresponding to the optimal selected transmit antennas
L_t	pilot symbols intervals
ξ_i	SNIR for the ith substream

List of Acronyms

MIMO	multiple-input multiple-output
SISO	single-input single-output
CSI	channel state information
MIMO-SM	multiple-input multiple-output spatial multiplexing
ML	maximum-likelihood
ZF	zero-forcing
MMSE	minimum mean squared-error
i.i.d.	independent and identically distributed
SIC	successive interference cancellation
OSIC	ordered SIC
DFD	decision-feedback detector
VBLAST	vertical Bell labs layered space-time
RF	radio-frequency
LNAs	low-noise amplifiers
ADCs	analog-to-digital converters
AS	antenna selection
BER	bit error rate
SNR	signal-to-noise ratio
H-ARQ	hybrid automatic-repeat-request
BLAST	Bell labs layered space-time
TITO	two-input two-output
MSI	multi-stream interference

DBLAST   diagonal Bell labs layered space-time

QAM   quadrature amplitude modulation

MUD   multiuser detection

QPSK   quaternary phase-shift keying

LOS   line-of-sight

PDF   probability density function

ZF-VBLAST   zero-forcing vertical Bell labs layered space-time

CDF   cumulative distribution function

GBN   go-back-n

ARQ   automatic-repeat-request

BPSK   binary phase-shift keying

SER   symbol error rate

V-SER   vector symbol error rate

PER   packet error probability

ISI   intersymbol interference

SNIR   signal-to-noise-plus-interference ratio

Chapter 1

Introduction

1.1 MIMO Communications

Communications over multiple-input multiple-output (MIMO) wireless channels have been a subject of intense research over the last decade, due to the rapid development of high-speed broadband wireless communication technologies. The use of multiple-antennas for both transmission and reception can drastically improve the wireless link performance through capacity and diversity gains, resulting in much more reliable wireless transmission relative to conventional single-input single-output (SISO) systems [1–3]. Specifically, Telatar [3] and Foschini [2] showed that, when the receiver but not the transmitter has perfect knowledge of the channel state information (CSI), the capacity of an independent Rayleigh distributed flat-fading channel will increase almost linearly with the minimum of the number of transmit and receive antennas. With this motivation an emerging MIMO signaling technique, referred to as spatial multiplexing, has been introduced in order to achieve a significant portion of the aforementioned promised theoretical capacity with reasonable implementation complexity [4]. Spatial multiplexing gain arises from transmitting independent data signals (parallel spatial data pipes) from the individual antennas. It is

1

worth highlighting that spatial multiplexing techniques achieve the linear increase in capacity in rich-scattering channels (uncorrelated fading). Keep in mind that MIMO systems also provide the traditional diversity gain (e.g., frequency/time/spatial) [5]. Thus MIMO signaling offers two different benefits: *i*) *high spectral efficiency* (linear increase in capacity), through spatial multiplexing, for no additional power or bandwidth expenditure [6]. This is realized by splitting the input data streams into multiple substreams for transmission over the different transmit antennas; *ii*) *diversity gain*, to combat deep channel fading, by transmitting multiple replicas of the same information signal over multiple independently fading paths. On the receiver side, this diversity is similar to that provided by the so-called RAKE receiver [5]. Also, diversity can be obtained with multiple transmit antennas using suitably designed transmit signals. The corresponding technique is referred to as space-time coding [7–9]. Note that it is possible to exploit these two benefits simultaneously, but there is a fundamental tradeoff between how much of each any scheme can get [10].

Given perfect channel knowledge at the receiver, various signal reception techniques for MIMO spatial multiplexing (MIMO-SM) systems, can be employed: *i*) *optimal maximum-likelihood* (ML) criterion. Note that, although the ML receiver is optimal, its complexity grows exponentially with the number of transmit antennas. Thereby, this fact makes the ML receiver impractical especially for systems with a large number of transmit antennas; *ii*) *linear suboptimal criteria* such as zero-forcing (ZF) or minimum mean squared-error (MMSE). It is well-known that MIMO-SM systems employing linear receivers are practically important due to their minimal complexity requirements. However, these detectors result in a loss in the diversity gain relative to the optimal ML detector [11]. For instance, in independent and identically distributed (i.i.d.) MIMO Rayleigh fading channels, with M transmit and N receive antennas, the use of ZF receiver achieves a diversity order of $N - M + 1$ [12], while the more complex ML detector achieves a diversity

order of N [13]; *iii) nonlinear suboptimal criteria* such as successive interference cancellation (SIC) or ordered SIC (OSIC), which have superior performance than both ZF and MMSE. One such receiver that employs SIC/OSIC is the decision-feedback detector (DFD) [14], which is also known in the MIMO literature as vertical Bell labs layered space-time (VBLAST) [15–17]. Specifically, the DFD uses SIC/OSIC to eliminate interference from different streams, which improves detection of transmitted symbols. Furthermore, the DFD is relatively simple to implement and can achieve a significant portion of the promised MIMO capacity.

1.2 Motivation

Along with aforementioned gains provided by MIMO systems, comes a price in hardware complexity [18,19], e.g., multiple analog radio-frequency (RF) chains. The RF chains normally comprise expensive hardware blocks such as low-noise amplifiers (LNAs), analog-to-digital converters (ADCs), and mixers at the transmitter and receiver end. This clearly presents a hardware challenge in terms of complexity and cost. To this end, antenna selection (AS) has been introduced as a means to mitigate this complexity problem, while exploiting the diversity provided by the transmit and receive antennas. The idea behind AS is to use only the optimal subset of antennas out of the available ones, thereby reducing the number of required RF chains [18,19]. Also, correlation at the transmit and/or receive antennas can potentially lead to a reduction in the MIMO system capacity [20]. In [20], the authors show that an increase in correlation coefficients results in capacity decrease, and when the correlation coefficients equal to unity, no advantage is provided by the MIMO channel. Therefore, investigation of such issues is important. Our contribution in this thesis is two-fold. First, we investigate the bit error rate (BER) performance of the ZF receiver over spatially correlated Ricean flat-fading channels. Second, we propose AS approaches for DFD in fading MIMO channels. The reason to focus on these problems is motivated as

follows.

1.2.1 BER Performance of ZF Receivers

In [12], the authors study the performance of the ZF receiver in Rayleigh fading channels with transmit correlation. Based on Wishart matrix analysis, the authors show that the ZF detector decomposes the MIMO system into M parallel streams with $N - M + 1$ diversity order. In [21], the performance of the ZF receiver is investigated over independent Ricean fading channels where an approximation for the average BER is given. Therefore, investigating the BER performance of the ZF receiver in spatially correlated Ricean flat-fading channels is an important issue. Moreover, the study of such receiver BER performance can be motivated in a number of ways as follows: i) the ZF receiver has low implementation complexity (simple receiver) which makes it practically important; ii) the independent Ricean fading model assumed in [21] is not ideal in practice. The spatial correlated Ricean flat-fading MIMO model is known to more accurately model real-world wireless environments [22]; iii) the ZF receiver performance approaches that of the MMSE at high signal-to-noise ratio (SNR) regime. Thus the derived BER expression can be used to model that of MMSE at high-SNR; iv) the study of ZF nulling technique provides a deep insight and understanding of the DFD, since the latter applies interference *nulling* and cancellation.

1.2.2 Transmit Antenna Selection for DFD

Recently, transmit and receive AS approaches, which maximize the capacity of uncorrelated Rayleigh flat-fading channels have been proposed in [23, 24]. The transmit AS approach presented in [23] makes use of an exhaustive search to find the optimal subset of transmit antennas out of the available ones. Therefore, an investigation into computationally efficient AS approaches is an important issue. Furthermore, the aforementioned capacity-based AS scheme is based on a general formula and is not specified to a specific

4

receiver. Thus this has motivated us to introduce a new pragmatic transmit AS approach for DFD that maximizes both the post-processing SNR at the receiver end, and the system capacity in uncorrelated Rayleigh flat-fading channels. It is shown that the proposed transmit AS scheme has performance comparable to optimal capacity-based selection based on exhaustive search [23], but with lower complexity.

1.2.3 Cross-Layer Based Transmit Antenna Selection for DFD

In [23–25], AS is studied from a physical layer point of view (e.g., capacity and error probability criteria). However, in practice, link quality is determined by both physical and data-link layers. A cross-layer approach that combines AS and adaptive modulation, in Rayleigh fading channels, is investigated in [26], where a hybrid automatic-repeat-request (H-ARQ) technique is used at the data-link layer to improve the link throughput. However, it is important to mention that the authors in [26] relied on assumptions that are too optimistic to be practical: *i*) uncorrelated signal propagation paths; *ii*) absence of direct-path propagation; *iii*) CSI perfectly known at the receiver. Only more recently, researchers realized the importance of these issues, where measurement results indicate that channels suffer from correlation [27]. The effects of Ricean fading on the capacity of multiple-antenna systems is examined in [28]. The authors show that Ricean fading can improve the capacity of a multiple-antenna system when the transmitter knows the Ricean factor. MIMO systems with Bell labs layered space-time (BLAST) [4] and orthogonal training signals have been investigated in [29], where it is shown that one generally spends half of the coherence interval training in order to maximize the throughput in a wireless channel. Motivated by the above observations, we further investigate the performance of a cross-layer based transmit AS for DFD over spatially correlated Ricean fading channels.

1.3 Summary of Contributions

The contribution of this thesis is two-fold. First, we investigate the BER performance of the ZF receiver over spatially transmit correlated Ricean flat-fading channels. Then two pragmatic AS approaches for the DFD over MIMO fading channels are presented. The primary contributions are summarized as follows:

- The BER performance of the ZF receiver over spatially transmit correlated Ricean flat-fading channels is investigated, where an approximation for the average BER of each substream is derived.

- The BER performance in receive correlated Ricean flat-fading channels is also addressed. It is observed that the performance, when $N = M$, is the same as that of transmit correlated Ricean flat-fading channels.

- A closed-form expression for the optimal transmit correlation coefficient, which achieves the maximum capacity (i.e., uncorrelated case) of two-input two-output spatial multiplexing (TITO-SM) systems, is presented.

- A transmit AS approach for the DFD over independent Rayleigh flat-fading channels is presented. The selected transmit antennas are those that maximize both the post-processing SNR at the receiver end, and the system capacity. We have found that the proposed transmit selection scheme has performance comparable to optimal capacity-based selection based on exhaustive search, but with much less complexity.

- An upper bound on the outage probability for the proposed transmit AS approach is also derived.

- A cross-layer based transmit AS scheme for the DFD over spatially correlated Ricean flat-fading MIMO channels is further presented. The selected transmit antennas are those that maximize the link layer throughput of correlated MIMO channels.

- A closed-form expression for the throughput of MIMO system, performing the cross-layer based transmit selection, with perfect channel estimation is derived. We further

analyze the system performance with pilot-aided channel estimation. In that, we derive a closed-form expression of the overall system throughput. It is observed that the optimal capacity-based AS approach is more robust to imperfect channel estimation. However, in all cases, the cross-layer based transmit selection scheme is able to outperform the capacity-based one.

1.4 Thesis Overview

The thesis is organized as follows. In Chapter 2, a description of the general uncoded MIMO-SM system model is first given. We further review various signal reception techniques for MIMO-SM systems including, linear, successive, and ML decoding which can be used to remove the effect of the channel and reassemble the transmitted substreams.

In Chapter 3, the BER performance of the ZF receiver over spatially transmit correlated Ricean flat-fading channels is investigated. In particular, an approximation for the average BER of each substream is derived. Furthermore, we investigate the system performance in receive correlated Ricean flat-fading channels. It is observed that the performance, when $N = M$, is the same as that of transmit correlated Ricean flat-fading channels. Then a closed-form expression for the optimal transmit correlation coefficient, which achieves the maximum capacity (i.e., uncorrelated case) of TITO-SM systems, is presented.

Chapter 4 introduces a transmit selection approach for the DFD over independent Rayleigh flat-fading channels. An upper bound on the outage probability for the proposed scheme at high-SNR regime is also derived.

In Chapter 5, we propose a cross-layer based transmit AS scheme for the DFD over spatially correlated Ricean flat-fading MIMO channels. We further analyze the system performance with pilot-aided channel estimation.

Finally, in Chapter 6 conclusions and future work are given.

Chapter 2

Receiver Architectures for MIMO Spatial Multiplexing Systems

2.1 Introduction

The challenges faced by any receiver, designed for spatial multiplexing systems, is to mitigate the presence of multi-stream interference (MSI) with reasonable implementation complexity. MSI occurs in spatial multiplexing because the different data streams occupy the same resources in time and frequency. To this end, many advanced signal processing reception techniques have been proposed in order to exploit the high spectral efficiency offered by MIMO channels [4, 16, 30–32].

This chapter focuses on receiver structures for spatial multiplexing systems and the corresponding performance-complexity tradeoff. An outline of this chapter is as follows. In Section 2.2, the general uncoded MIMO-SM system model is presented. Section 2.3 discusses different receiver architectures, for spatial multiplexing, including the optimal ML receiver, suboptimal linear receivers (i.e., ZF and MMSE), and suboptimal nonlinear SIC/OSIC receivers. For the sake of completeness, Section 2.4 offers few important remarks. Finally, Section 2.5 concludes this chapter.

8
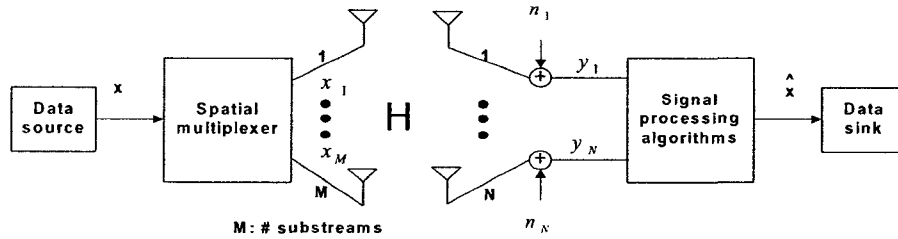
Figure 2.1: Schematic representation of the general uncoded MIMO-SM communication model.

2.2 General MIMO Spatial Multiplexing Model

Understanding the general MIMO-SM system model and its different receiver architectures are crucial to the analysis of the ZF receiver, and also to the development of appropriate AS schemes. In this section, we describe the general uncoded MIMO-SM system model. In that, we state the input-output relationship for the aforementioned model.

Consider a single-user point-to-point MIMO-SM system with M transmit and N ($N \geq M$) receive antennas as illustrated in Fig. 2.1. The incoming data is fed into a spatial multiplexer (serial-to-parallel converter) that converts the input data stream into M independent parallel substreams. Next, the substreams are independently mapped to produce the M-dimensional symbol vector x. In general, it is assumed that the transmitted substreams have uniform power. At the receiver end, various signal processing reception techniques can be employed such as ML, ZF, MMSE, and SIC/OSIC as, for example, in the case of DFD [14].

The sampled received baseband signal can be represented as

$$y = Hx + n, \tag{2.1}$$

where $\mathbf{x} = [x_1, x_2, \ldots, x_M]^T$ is the ($M \times 1$) transmitted signal vector with x_i ($1 \leq i \leq M$) belonging to a finite constellation set $\mathcal{A}$. The superscript $(\cdot)^T$ denotes transpose. $\mathbf{y} =$

9

$[y_1, y_2, \ldots, y_N]^T$ is the $(N \times 1)$ received signal vector, $\mathbf{n} = [n_1, n_2, \ldots, n_N]^T$ is the $(N \times 1)$ received noise vector, and

$$\mathbf{H} = \begin{bmatrix} h_{11} & h_{12} & \ldots & h_{1M} \\ h_{21} & h_{22} & \ldots & h_{2M} \\ \vdots & \vdots & \ddots & \vdots \\ h_{N1} & h_{N2} & \ldots & h_{NM} \end{bmatrix}, \tag{2.2}$$

is the $(N \times M)$ MIMO channel matrix, with h_{ij} representing the complex gain of the channel between the jth transmit antenna and the ith receive antenna for $1 \le i \le N$, $1 \le j \le M$. The entries of $\mathbf{H}$ are i.i.d. and circularly symmetric complex Gaussian random variables with mean μ and unit-variance, i.e., $h_{ij} \sim CN(\mu, 1)$. Depending on $\mu = 0$ or $\mu \neq 0$, the channel is Rayleigh or Ricean distributed, respectively. Note that in general the channel gains may be correlated [20, 27]. $\mathbf{H}$ is assumed to be known to the receiver to allow coherent detection, but not at the transmitter. We assume that the channel is flat-fading and quasi-static, where the fading coefficients are constant over the entire frame and vary independently from one frame to another. Furthermore, perfect synchronization and timing at the receiver are assumed. The receiver noise $\mathbf{n} \sim CN(0, N_0 \mathbf{I}_N)$ consists of independent circularly symmetric zero-mean complex Gaussian entries of variance N_0, where $\mathbf{I}_N$ is an identity matrix of size N. Denote $P_x \triangleq \mathbb{E}[\mathbf{x}^H \mathbf{x}]$ as the total average energy over a symbol period (i.e., total input power), where $\mathbb{E}[\cdot]$ stands for expectation, and $(\cdot)^H$ is the conjugate transpose. Thus the input SNR is defined as

$$\zeta = \frac{P_x}{N_0}. \tag{2.3}$$

2.3   Receivers for Spatial Multiplexing Systems

The aforementioned MIMO signaling promise spurred researchers to implement suitable advanced signal processing reception algorithms that achieve a large portion of the theoretical promised potential. Among which is the VBLAST [15–17], a simplified version of the diagonal Bell labs layered space-time (DBLAST) [4]. VBLAST can achieve a large fraction of the theoretical MIMO capacity with a reasonable implementation complexity. Using *successive interference nulling and cancellation*, VBLAST can eliminate MSI and detect the transmitted data at substream basis. The remainder of this section focuses on receiver structures for spatial multiplexing and the corresponding performance-complexity tradeoff.

2.3.1   ML Receiver

The ML receiver is optimal in terms of the BER. Let $\mathcal{A}$ be the symbol constellation set of size $\mathcal{M}$ (e.g., $\mathcal{M}$-ary quadrature amplitude modulation ($\mathcal{M}$-QAM)). Assuming equally likely vector symbols $\mathbf{x}$, the ML receiver forms its estimate of $\mathbf{x}$ according to

$$\hat{\mathbf{x}} = \arg\min_{\mathbf{x}\in\mathcal{A}^M}\|\mathbf{y} - \mathbf{H}\mathbf{x}\|^2, \tag{2.4}$$

where $\hat{(\cdot)}$ is the data estimate, and $\|\cdot\|$ denotes Frobenius norm. Examining (2.4) reveals that the ML receiver suffers from complexity issue, in the sense that the minimization problem is performed over $|\mathcal{A}|^M$ possible transmitted symbols. This renders the decoding complexity exponential in the number of transmit antennas $\left(\text{i.e.,} O\left(\mathcal{M}^M\right)\right)$. Thereby, the ML detector is impractical to many real-life applications (especially when M is large). For instance, if 16-QAM is adopted with $M = 6$ transmit antennas, the ML detector needs to search over $16^6 = 16,777,216$ symbols!. This has motivated the search for practical suboptimal receivers which are relatively simple to implement and powerful in terms of

11

BER performance. Among which is the VBLAST which can utilize a layered architecture and applies successive interference nulling and cancellation by splitting the channel vertically [15–17]. The details of the algorithm will be presented later. Note that a search technique with $O\left(\mathcal{M}^3\right)$ complexity, referred to as sphere decoding has been proposed in [33].

2.3.2 Linear Receivers

Linear receivers are the simplest spatial multiplexing receivers since they only require a matrix multiplication to separate the substreams. Thus they are practically important especially for systems which have large number of transmit and receive antennas. As depicted in Fig. 2.2, the received signal vector $\mathbf{y}$ is linearly transformed by a matrix equalizer $\mathbf{G}$ which basically eliminates the effects of the channel to get

$$
\begin{aligned}
\mathbf{r} &= \mathbf{G}\mathbf{y} \\
&= \mathbf{G}\mathbf{H}\mathbf{x} + \mathbf{G}\mathbf{n}.
\end{aligned}
\tag{2.5}
$$

Then (2.5) is quantized to get an estimate of the transmitted symbol vector $\hat{\mathbf{x}} = C(\mathbf{r})$, where C stands for mapping to the nearest point in the symbol constellation (slicer). Inspection of (2.5) reveals that $\mathbf{G}$ colors the noise (i.e., noise power is a function of channel). The matrix equalizer can be computed according to different criteria such as ZF and MMSE. The details of the ZF and MMSE criteria are given below.
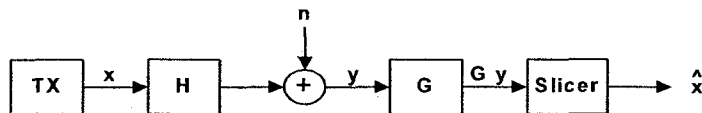
Figure 2.2: Schematic representation of linear receiver front-ends.

ZF receiver: For the ZF criterion, the matrix equalizer is given by

$$\mathbf{G}_{\text{ZF}} = \mathbf{H}^{\dagger}, \tag{2.6}$$

where $\mathbf{H}^{\dagger} = \left(\mathbf{H}^{H}\mathbf{H}\right)^{-1}\mathbf{H}^{H}$ denotes the Moore-Penrose pseudoinverse of the channel matrix $\mathbf{H}$. Substituting (2.6) in (2.5), and using $\mathbf{H}^{\dagger}\mathbf{H} = \mathbf{I}_M$ where $\mathbf{I}_M$ is an identity matrix of size M, the output of the ZF receiver can be expressed as

$$\mathbf{r} = \mathbf{x} + \mathbf{H}^{\dagger}\mathbf{n}. \tag{2.7}$$

It can bee readily seen that the ZF receiver eliminates MSI entirely, however, at the expense of enhancing the additive noise. Also, the ZF receiver decomposes the MIMO system into M parallel streams with additive spatially-colored noise, where each stream achieves $N - M + 1$ diversity order [12, 34]. To conclude, although the ZF criterion has a low implementation complexity, it yields the following two problems: i) It attempts to invert the channel, but amplifies the noise in the process; ii) the criterion can encounter singular matrices that are not invertible.

MMSE receiver: The MMSE receiver front-end, $\mathbf{G}_{\text{MMSE}}$, balances MSI mitigation (i.e., invert channel) with noise enhancement in a MMSE sense, and is given by

$$\mathbf{G}_{\text{MMSE}} = \left(\mathbf{H}^{H}\mathbf{H} + \gamma_0^{-1}\mathbf{I}_M\right)^{-1}\mathbf{H}^{H}, \tag{2.8}$$

where $\gamma_0 = \zeta/M$ is the average normalized SNR at each receive antenna. Using (2.8) one can see that, at low-SNR regime (i.e., $\gamma_0 \ll 1$), the MMSE receiver outperforms the ZF receiver and approaches the matched-filter one. In this case, $\mathbf{G}_{\text{MMSE}}$ can be expressed as

$$\mathbf{G}_{\text{MMSE}} = \gamma_0\mathbf{H}^{H}. \tag{2.9}$$

13

Whereas, at high-SNR regime (i.e., $\gamma_0 \gg 1$), $\mathbf{G}_{MMSE}$ is given by

$$\mathbf{G}_{MMSE} = \mathbf{G}_{ZF}. \tag{2.10}$$

Thus, at high-SNR, MMSE and ZF have asymptotically the same post-processing SNR with $N - M + 1$ diversity order for each stream. To conclude, MMSE receiver minimizes the error due to the noise and the interference combined. In addition, although ML receivers have superior performance, linear receivers offer a significant computational reduction.

2.3.3 SIC Receivers

The nonlinear SIC criterion has been first introduced in the theory of multiuser detection (MUD) [35,36]. The key idea in SIC receivers centers around peeling of layers, where the input data streams are sequentially detected and stripped layer-by-layer. In what follows, we briefly review the nonlinear SIC reception technique.

Before proceeding further, let us first write $\mathbf{H}$ in its column-wise matrix form as $\mathbf{H} = [\mathbf{h}_1, \mathbf{h}_2, \ldots, \mathbf{h}_M]$, where $\mathbf{h}_i$ denotes the ith $(1 \leq i \leq M)$ column of $\mathbf{H}$. Consequently, (2.1) can be rewritten as

$$\mathbf{y} = \sum_{i=1}^{M} \mathbf{h}_i x_i + \mathbf{n}. \tag{2.11}$$

Without loss of generality, we assume that the SIC receiver first estimates the signal with the spatial structure $\mathbf{h}_1$ (i.e., x_1). Now rewrite (2.11) as

$$
\begin{aligned}
\mathbf{y} &= \sum_{i=1}^{M} \mathbf{h}_i x_i + \mathbf{n} \\
&= \mathbf{h}_1 x_1 + \left(\sum_{i=2}^{M} \mathbf{h}_i x_i + \mathbf{n} \right),
\end{aligned} \tag{2.12}
$$

where the first term is the target signal, and the second is the interference plus noise. The signal estimator can be either ZF or MMSE estimator. Suppose that ZF estimator

14

is adopted, then we find a weight vector $\mathbf{w}_1$ such that

$$\mathbf{w}_1^H \mathbf{h}_1 = \delta, \qquad (2.13)$$

where δ is Dirac's delta. Now multiply (2.12) by $\mathbf{w}_1^H$, we get the decision statistic for x_1

$$d_1 = \mathbf{w}_1^H \mathbf{y}. \qquad (2.14)$$

Slicing d_1, we get an estimate of x_1

$$\hat{x}_1 = C(d_1). \qquad (2.15)$$

Upon detection of x_1, its contribution to the received vector $\mathbf{y}$ is totally subtracted under the assumption that $\hat{x}_1 = x_1$. After subtracting the contribution of $x_1, \ldots, x_k$, we can write the updated received vector as

$$\mathbf{y}^{(k)} = \mathbf{y} - \sum_{i=1}^{k} \mathbf{h}_i \hat{x}_i. \qquad (2.16)$$

Thus the received vector after canceling the effect of x_1 is

$$
\begin{aligned}
\mathbf{y}^{(1)} &= \mathbf{y} - \mathbf{h}_1 \hat{x}_1 \\
&= \sum_{i=2}^{M} \mathbf{h}_i x_i + \mathbf{n} \\
&= \mathbf{h}_2 x_2 + \left(\sum_{i=3}^{M} \mathbf{h}_i x_i + \mathbf{n} \right).
\end{aligned}
\qquad (2.17)
$$

Similarly the algorithm estimates the signal with spatial structure $\mathbf{h}_2$ (i.e., x_2). The process continues until x_M has been detected as depicted in Figs. 2.3(a) and 2.3(b).

Now it is essential to mention that the detection of x_2 is more reliable than that of x_1, and so on. The reason is that to estimate x_1 the receiver needs to null out $M - 1$ interferences

15
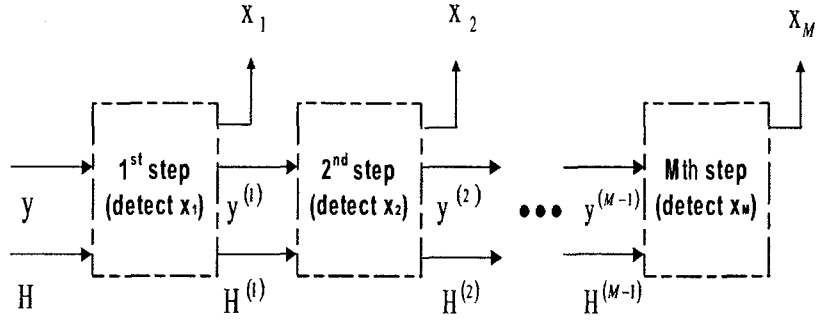
(a) The process of the nonlinear SIC reception technique.
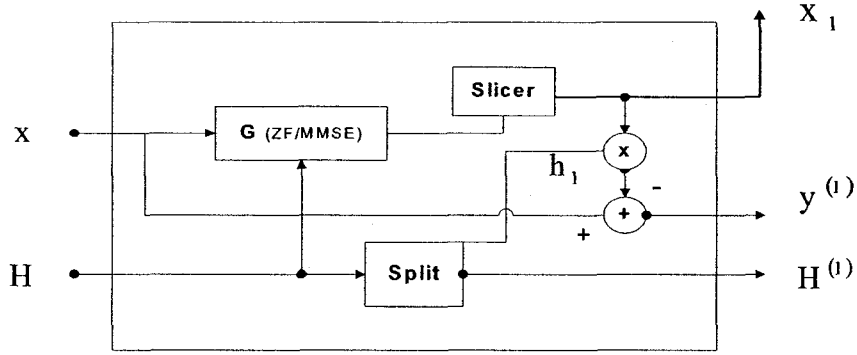
(b) First step of SIC technique.

Figure 2.3: Nonlinear SIC receiver architecture.

with spatial structure vectors $\mathbf{h}_2, \mathbf{h}_3, \ldots, \mathbf{h}_M$ $\left(\text{i.e., } \sum_{i=2}^{M} \mathbf{h}_i x_i \right)$, which consumes $M-1$ degrees of freedom. Whereas to detect x_2, the receiver only needs to null out the remaining $M-2$ interferences (see (2.17)). Hence, intuitively the detection of x_2 is more reliable than that of x_1 and so on. It is known that in an i.i.d. Rayleigh flat-fading channel, the ith detected substream has a diversity order of $D_i = N - M + i$ with $1 \leq i \leq M$ [5]. Ignoring the propagation of error (i.e., perfect feedback), SIC receivers decouple the MIMO channel into a set of M independent, one-dimensional (SISO) parallel virtual subchannels. However, error propagation exists and can seriously degrade the overall performance of SIC receivers. To conclude, complexity of SIC receivers is high compared to linear receivers, but SIC receivers outperform the linear ones.

16

2.3.4 OSIC Receivers

As already pointed out, detection error of the first substream can seriously influence detection of the subsequent substreams. Thus, the first detected substream is the bottleneck which limits the overall performance of SIC receivers. To improve SIC performance the streams can be reordered based on SNR at each stage. This ordering is equivalent to the global maximization of the minimum substream SNR [15–17]. Such receivers are referred to as OSIC receivers (e.g., VBLAST). It is shown in [37] that for an i.i.d. Rayleigh distributed fading channel with two transmitting antennas ($M = 2$), the optimal ordering does not result in increased diversity but only in a fixed SNR gain. Later, the authors in [38] showed that the diversity gain of VBLAST with optimal ordering is $N - M + 1$. That is applying optimal ordering does not help improve the diversity gain of VBLAST [38]. The interested reader is referred to [15–17,37–42] for further details on VBLAST algorithm. In what follows, we briefly describe its key points.

At the transmitter, VBLAST demultiplexes the high-rate input data streams into M lower-rate independent substreams for transmission over the M available transmit antennas (at the same time and frequency). This horizontal layering eliminates the space time wastage, but loses the transmit diversity. At the receiver side, each of the N antennas receive all transmitted substreams which are mixed and superimposed with thermal noise. Using OSIC, VBLAST demultiplexes and detects the transmitted data at substream basis. The signal estimator can be either ZF or MMSE estimator. VBLAST is shown to be able to achieve about 72% of the capacity [16]. The reason is that imposing same rate of transmission makes the channel capacity limited by the worst of the M subchannels. As pointed out above, at each step, VBLAST detects the component of the transmitted vector x which has the largest post-processing SNR (optimal ordering). Without loss of generality, we assume that $[k_1, k_2, \ldots, k_M]$ denote the optimal ordering permutation of $[1, 2, \ldots, M]$. For notational convenience, we use y_1 instead of y (defined in (2.1)). Now the VBLAST

17

detection algorithm can be summarized as follows:

Initialization:

$$\mathbf{G}_1 = \mathbf{H}^\dagger \qquad (2.18a)$$

$$i = 1 \qquad (2.18b)$$

Recursion:

$$k_i = \underset{j \ni \{k_1,\ldots,k_{i-1}\}}{\arg\max} \, \| (\mathbf{G}_i)_j \|^2 \qquad (2.18c)$$

$$\mathbf{w}_{k_i} = (\mathbf{G}_i)_{k_i} \qquad (2.18d)$$

$$y_{k_i} = \mathbf{w}_{k_i} \mathbf{y}_i \qquad (2.18e)$$

$$\hat{x}_{k_i} = C\left(y_{k_i}\right) \qquad (2.18f)$$

$$\mathbf{y}_{i+1} = \mathbf{y}_i - \hat{x}_{k_i} (\mathbf{H})_{k_i} \qquad (2.18g)$$

$$\mathbf{G}_{i+1} = \mathbf{H}^\dagger_{\overline{k}_i} \qquad (2.18h)$$

$$i = i + 1 \qquad (2.18i)$$

where $(\mathbf{G}_i)_j$ is the jth row of $\mathbf{G}_i$, $\mathbf{H}_{\overline{k}_i}$ denote the matrix obtained by zeroing the columns $k_1, k_2, \ldots, k_i$ of $\mathbf{H}$. (2.18c) determines the optimal ordering by choosing the minimum-norm row of $\mathbf{G}_i$. Nulling and estimation steps are performed in (2.18e) and (2.18f), respectively. Interference cancellation (decision-feedback) is performed in (2.18g). Finally (2.18h) computes the new Moore-Penrose pseudoinverse for the next iteration.

Example: To numerically investigate the performance of VBLAST, we consider a single-user point-to-point $(M = 2, N = 2)$ MIMO-SM system. We assume that symbols on all substreams are derived from the uncoded quaternary phase-shift keying (QPSK) signal constellation set $\mathcal{A} = \{1 \pm i, \pm 1 + i\}$. The entries of the noise vector $\mathbf{n}$ are i.i.d. with zero-mean and variance $N_0 = 0.2512$, i.e., $\mathbf{n} \sim CN(0, 0.2512 \mathbf{I}_N)$. $\mathbf{H}$ is assumed to be independent Rayleigh distributed with entries $h_{ij} \sim CN(0, 1)$. The propagation channel matrix

18

H is given by

$$\mathbf{H} = \begin{bmatrix} -0.3059 - 0.8107i & 0.0886 + 0.8409i \\ -1.1777 + 0.8421i & 0.2034 - 0.0266i \end{bmatrix}.$$

The data and noise vectors are given respectively by

$$\mathbf{x} = \begin{bmatrix} 1+i \\ -1-i \end{bmatrix} \quad \text{and} \quad \mathbf{n} = \begin{bmatrix} 0.1160 - 0.0662i \\ 0.0619 + 0.2572i \end{bmatrix}.$$

Using (2.1), the received vector **y** is

$$\mathbf{y} = \begin{bmatrix} 1.3731 - 2.1123i \\ -2.1879 - 0.2552i \end{bmatrix}.$$

The Moore-Penrose pseudoinverse $\mathbf{H}^\dagger$ can be written as

$$\mathbf{H}^\dagger = \begin{bmatrix} 0.1157 - 0.1570i & -0.6348 - 0.4928i \\ 0.1979 - 1.3617i & -0.7572 - 0.3239i \end{bmatrix}.$$

Interference nulling step (1st iteration): Using (2.18a), we get

$$\mathbf{G}_1 = \mathbf{H}^\dagger = \begin{bmatrix} 0.1157 - 0.1570i & -0.6348 - 0.4928i \\ 0.1979 - 1.3617i & -0.7572 - 0.3239i \end{bmatrix}.$$

Now, we need to find which symbol we have to detect first. According to (2.18c), the optimal ordering is to select the minimum-norm row of $\mathbf{G}_i$ ($1 \leq i \leq M$). Since $\| (\mathbf{G}_1)_1 \|^2 = 0.8270$ and $\| (\mathbf{G}_1)_2 \|^2 = 1.6037$, therefore we get $k_1 = 2$. Using (2.18e), VBLAST first

19

estimates x_2 (2nd subchannel) as

$$y_2 = \begin{bmatrix} 0.1979 - 1.3617i & -0.7572 - 0.3239i \end{bmatrix} \begin{bmatrix} 1.3731 - 2.1123i \\ -2.1879 - 0.2552i \end{bmatrix} = -1.0307 - 1.3858i.$$

Now slicing y_2, we get an estimate $\hat{x}_2 = -1 - i$.

Interference cancellation step (1st iteration): Upon detection of x_2, its contribution to the received vector is subtracted. The modified received vector $\mathbf{y}_2$ is then

$$\mathbf{y}_2 = \mathbf{y}_1 - \hat{x}_2 (\mathbf{H})_2 = \begin{bmatrix} 0.6208 - 1.1828i \\ -1.9579 - 0.0784i \end{bmatrix}.$$

The matrix $\mathbf{H}_{\bar{2}}$ can be written as

$$\mathbf{H}_{\bar{2}} = \begin{bmatrix} -0.3059 - 0.8107i & 0 \\ -1.1777 + 0.8421i & 0 \end{bmatrix}.$$

Thus the new Moore-Penrose pseudoinverse for the next epoch is

$$\mathbf{G}_2 = \begin{bmatrix} -0.1074 + 0.2848i & -0.4137 - 0.2958i \\ 0 & 0 \end{bmatrix}.$$

Interference nulling step (2nd iteration): Directly, we have $k_2 = 1$ (last layer to detect). Then

$$y_1 = \begin{bmatrix} -0.1074 + 0.2848i & -0.4137 - 0.2958i \end{bmatrix} \begin{bmatrix} 0.6208 - 1.1828i \\ -1.9579 - 0.0784i \end{bmatrix} = 1.0569 + 0.9154i,$$

and the corresponding estimate is $\hat{x}_1 = 1 + i$.

20

Now, the algorithm stops and the estimated transmitted signal vector $\hat{\mathbf{x}}$ is

$$\hat{\mathbf{x}} = \begin{bmatrix} 1+i \\ -1-i \end{bmatrix}.$$

It can be readily seen that it is indeed the correct estimate of $\mathbf{x}$.

2.4 Further Remarks

For the sake of completeness, in this section we make a few brief remarks.

Remark 1: A coded architecture namely Turbo-BLAST has been proposed in [31]. The new transceiver has less computational complexity than the optimal ML decoder. Furthermore, it has a probability of error performance that is order of magnitude smaller than the traditional BLAST architecture [31].

Remark 2: DBLAST is the most complex algorithm of the BLAST architecture. Then probably comes the Turbo-BLAST, and the the simplest one is VBLAST.

Remark 3: BLAST architecture achieves its best performance in rich-scattering channels [4]. Thus, spatial correlation limits the performance of BLAST transceivers.

Remark 4: ZF, MMSE, SIC, and OSIC receivers provide only $N - M + 1$ diversity order, but have varying SNR loss (see Table. 2.1). Thus, with $N = M$, the diversity performance for linear receivers is exactly the same as that of SISO system! Therefore, the use of suboptimal receivers incur a loss in the diversity order. This is in contrast to the more complex ML receiver for which the diversity order is always N [13]. However, SIC/OSIC receivers have the lowest SNR loss among all suboptimal receivers.

Table 2.1: Comparison of spatial multiplexing receivers

	ZF	MMSE	SIC/OSIC	ML
Diversity order	N-M+1	N-M+1	N-M+1	N
SNR loss	High	Low	Low	Zero

2.5 Conclusions

In this chapter, we have provided an overview of different receivers for spatial multiplexing systems and the corresponding performance-complexity tradeoff. In Section 2.2, we have presented the general model of a typical uncoded MIMO-SM system model. In Section 2.3, various receiver architectures for spatial multiplexing systems have been introduced. In particular, we have demonstrated that the ML detector provides the optimal BER performance, but it suffers from exponential complexity issue. This fact makes it impractical to many real-life scenarios. Thereby, linear and SIC/OSIC receivers were introduced as a tradeoff between performance and computational complexity. In that, we have discussed VBLAST algorithm and provided a numerical example for clarification purposes.

Chapter 3

Performance of Zero-Forcing Detectors over Spatially Correlated Ricean MIMO Channels

3.1 Introduction

As pointed out in Chapter 1, MIMO-SM systems have recently received significant attention due to the extraordinary high spectral efficiency they provide in wireless communication systems [2,3]. In Chapter 2, we have demonstrated that spatial multiplexing systems employing ZF receivers are practically important due to their minimal complexity requirements. However, some impairments, such as correlation, at the transmit and/or receive antennas may lead to substantial degradation in the system performance [27,43,44]. With this motivation, in this chapter, we study the BER performance of the ZF receiver over transmit correlated Ricean flat-fading channels.

3.1.1 Prior Work

In [12], the authors study the performance of the ZF receiver in Rayleigh fading channels with transmit correlation. Based on Wishart matrix analysis, the authors show that the ZF detector decomposes the MIMO system into M parallel streams with $N - M + 1$ diversity order. In [21], the performance of the ZF receiver is investigated over independent Ricean fading channels where an approximation for the average BER is given.

3.1.2 Contributions and Organization

In this chapter, we investigate the BER performance of the ZF receiver over transmit correlated Ricean flat-fading channels. The focus on correlated Ricean channels can be motivated in a number of ways as follows: i) the authors in [21] assume that the subchannels fade independently. However, in real propagation environments, fading signals are not independent where measurement results indicate that the channels suffer from correlation [27, 43, 44]. Therefore, the independent Ricean fading model assumed in [21] is not ideal in practice, especially for systems that have poor scattering conditions and/or insufficient spacing between adjacent antennas; ii) this channel model is known to be an appropriate model for wireless propagation environments [22]; iii) the derived average BER expression can be used to model the MMSE performance at high-SNR.

In this chapter the performance of the ZF receiver over transmit correlated Ricean flat-fading channels is presented. A widely accepted mathematical model for correlated fading channels is presented in [45–48]. Their common approach is to model the correlation at the receiver and at the transmitter independently, neglecting the statistical interdependence of both links. Thus correlation is determined as the product of a receive-side and transmit-side components. This allows one to write the channel matrix in a simple format based on two constant correlation matrices plus an inner matrix of i.i.d. circularly symmetric complex Gaussian random variables. Furthermore, in our work, we constrain our analysis to the

M: # substreams
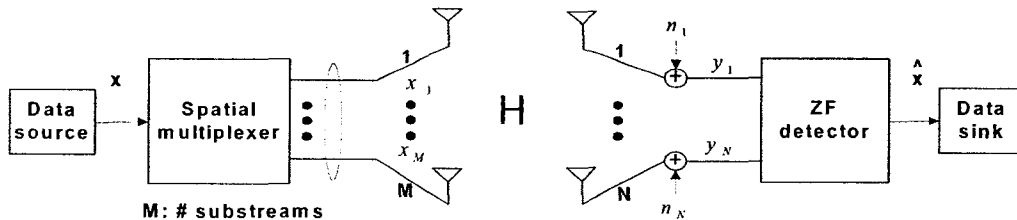
Figure 3.1: MIMO-SM system employing ZF receiver.

exponential correlation model [49]. This model is physically realistic since correlation decreases with increasing distances between antennas. In that, we derive an approximation for the average BER when QPSK modulation is used with each transmitted substream. Moreover, we investigate the system performance in receive correlated Ricean flat-fading channels. We further derive a closed-form expression for the optimal correlation coefficient that maximizes the capacity (i.e., uncorrelated case) of TITO-SM systems.

This chapter is organized as follows. System model is introduced in Section 3.2. Performance analysis is presented in Section 3.3. Section 3.4 presents simulation results to assess the accuracy of our analytical results. Finally, conclusions are given in Section 3.5.

3.2 System Model

Consider a point-to-point single-user MIMO-SM system that employs M transmit and $N (N \geq M)$ receive antennas, and a $1 : M$ spatial multiplexer as shown in Fig. 3.1. The system works as follows. At one symbol time, M input symbols are multiplexed to produce the M-dimensional symbol vector x for transmission over all M antennas. Then the data vector x is sent through the channel, which is assumed to be flat-fading and slowly-time varying. At the receiver side, the antennas receive the M substreams which are mixed and superimposed by noise. Upon reception the ZF receiver is used to detect the transmitted data.

25

The corresponding sampled received baseband signal is given by

$$y = Hx + n, \qquad (3.1)$$

where $y \in C^{N \times 1}$ is the received signal, $H \in C^{N \times M}$ is the spatially correlated Ricean channel matrix. We assume that the receiver has a perfect knowledge of the channel matrix H. The information vector $x \in C^{M \times 1}$ consists of independent and uniform power transmitted substreams. The receiver noise $n \sim CN(0, N_0 I_N)$ consists of independent circularly symmetric zero-mean complex Gaussian entries of variance N_0.

For the sake of simplicity, we assume the receiver to be located at a richly-scattered propagation environment so that the fading at the receiver is spatially uncorrelated while the transmitter is located at a high altitude, and therefore the fading is only transmit correlated. This scenario is typical in the down-link channel in mobile communication systems. Accordingly, the elements of each row of the channel matrix H are correlated and for each row, we can write

$$R_t = \mathbb{E}\left[h_i^H h_i\right], \qquad \text{for} \quad i = 1, 2, \ldots, N, \qquad (3.2)$$

where R_t and h_i are the $M \times M$ transmit nonnegative semidefinite (Hermitian) correlation matrix, and the ith row of H, respectively. Note that the former can be represented as $R_t = R_t^{1/2} R_t^{H/2}$ (Cholesky factorization).

The Ricean channel matrix H is composed of two components; the line-of-sight (LOS) component (deterministic and constant), and a component resulting from multipath propagations (randomly varying). Hence, the channel matrix H that, contains transmit antenna correlation but no receive correlation, is given by [50]

$$H = \bar{H}_{LOS} + \bar{H}_w R_t^{1/2}, \qquad (3.3)$$

26

where

$$\bar{\mathbf{H}}_{\text{LOS}} = \sqrt{\frac{\kappa}{\kappa+1}}\,\mathbf{H}_{\text{LOS}} \quad \text{and} \quad \bar{\mathbf{H}}_w = \sqrt{\frac{1}{\kappa+1}}\,\mathbf{H}_w. \tag{3.4}$$

The $N \times M$ matrix $\bar{\mathbf{H}}_w$ consists of i.i.d. circularly symmetric Gaussian random variables with zero-mean and unit-variance $\sim CN(0,1)$. $\bar{\mathbf{H}}_{\text{LOS}} \triangleq \mathbb{E}[\mathbf{H}]$ represents the channel mean and κ defines the Ricean factor, which indicates the strength of the LOS component relative to the multipath component. Following the definition in [51], we can readily see that

$$\kappa = \frac{\|\bar{\mathbf{H}}_{\text{LOS}}\|^2}{\mathbb{E}\left[\|\mathbf{H} - \bar{\mathbf{H}}_{\text{LOS}}\|^2\right]}. \tag{3.5}$$

Moreover, we assume that the transmitter and receiver are positioned far from each other which is always the case in many practical applications [52]. Consequently, the channel can be approximated by

$$\mathbf{H} = \sqrt{\frac{\kappa}{\kappa+1}}\,e^{j\theta}\,\Psi_{N,M} + \sqrt{\frac{1}{\kappa+1}}\,\mathbf{H}_w\,\mathbf{R}_t^{1/2}, \tag{3.6}$$

where $\Psi_{N,M}$ denotes the $N \times M$ matrix of all ones. It is reasonable to consider $\theta = \pm \pi/4$, with $e^{j\theta} = \left(\frac{1+j}{\sqrt{2}}\right)$, which indicates an equal power of LOS component per dimension of the $\mathbf{H}$ entries [52]. Hence, $\mathbf{H} \sim CN(\mathbf{M}, \mathbf{I}_N \otimes \Sigma)$ with $\mathbf{M} = \mathbb{E}[\mathbf{H}] = \sqrt{\frac{\kappa}{\kappa+1}}\left(\frac{1+j}{\sqrt{2}}\right)\Psi_{N,M}$, and $\Sigma = \mathbf{R}_t\,\mathbf{I}_M$ is the covariance matrix of $\mathbf{H}$, and $\otimes$ denotes the Kronecker product of matrices.

As previously disclosed, we constrain our discussion to the exponential correlation model [49]. For this model, the entries of the transmit correlation matrix, $\mathbf{R}_t$, are given by

$$[\mathbf{R}_t]_{i,j} = \begin{cases} \rho^{j-i}, & i \leq j \\ \\ [\mathbf{R}_t]^*_{j,i}, & i > j \end{cases}, \quad |\rho| \leq 1, \tag{3.7}$$

27

where $(\cdot)^*$ denotes complex conjugate and ρ is the complex correlation coefficient of neighboring transmit branches. Based on (3.7), we write $\mathbf{R}_t$ in its matrix form as

$$
\mathbf{R}_t = \begin{bmatrix} 1 & \rho & \rho^2 & \cdots & \rho^{M-1} \\ \rho^* & 1 & \rho & \ddots & \vdots \\ \rho^{*2} & \rho^* & 1 & \ddots & \rho^2 \\ \vdots & \ddots & \ddots & \ddots & \rho \\ \rho^{*M-1} & \cdots & \rho^{*2} & \rho^* & 1 \end{bmatrix}.
\tag{3.8}
$$

Inspection of (3.8) discloses that the correlation decreases with increasing the distance between transmit antennas.

3.3   Performance Analysis

In this section we derive an approximation for the average BER performance of the ZF receiver in transmit correlated Ricean flat-fading channels. Moreover, a closed-form expression for the optimal transmit correlation coefficient, which achieves the maximum capacity (i.e., uncorrelated case) of TITO-SM systems, is presented.

3.3.1   BER of ZF Receiver over Correlated Ricean Channels

The performance of spatial multiplexing with linear detectors is a function of the effective SNR, denoted by γ_k, for each stream with $k = 1, 2, \ldots, M$, after linear processing. From [25], the post-processing SNR of the kth stream for the ZF receiver is given by

$$
\gamma_k = \frac{\gamma_0}{[\mathbf{H}^H \mathbf{H}]_{kk}^{-1}},
\tag{3.9}
$$

where $\gamma_0 = \zeta/M$, is the average normalized received SNR at each receive antenna, and $\left[\mathbf{H}^H \mathbf{H}\right]_{kk}^{-1}$ is the (k,k)th element of matrix $\left[\mathbf{H}^H \mathbf{H}\right]^{-1}$.

Now if we define

$$\mathbf{W} = \mathbf{H}^H \mathbf{H}, \tag{3.10}$$

then $\mathbf{W}$ is always an $M \times M$ square matrix. It is known that when $\mathbf{H}$ is a complex normally distributed matrix as described above, the distribution of $\mathbf{W}$ is given by the non-central Wishart distribution [28, 53]. Note that here we use the shorthand notation $\mathbf{W} \sim CW_M(N, \Sigma)$ to denote a central Wishart distribution, which results when the elements of $\mathbf{H}$ are zero-mean Gaussian random variables, with N degrees of freedom (sample size) and where Σ is the Hermitian covariance matrix of the columns (assumed to be the same for all columns). The subscript M explicitly denotes the sample matrix. Also, the shorthand notation $\mathbf{W} \sim CW_M\left(N, \Sigma, \Sigma^{-1}\mathbf{M}\mathbf{M}^H\right)$ denotes the non-central Wishart distribution with N degrees of freedom, which results when the elements of $\mathbf{H}$ are Gaussian random variables with $\mathbf{M} = \mathbb{E}[\mathbf{H}] \neq \mathbf{0}$, where $\mathbf{0}$ denotes a zero matrix.

Here we approximate the non-central Wishart distribution $\mathbf{W} \sim CW_M\left(N, \Sigma, \Sigma^{-1}\mathbf{M}\mathbf{M}^H\right)$ by a central Wishart distribution $\mathbf{W}' \sim CW_M\left(N, \Sigma + \frac{1}{N}\mathbf{M}^H\mathbf{M}\right)$ as in [21]. This technique represents a non-central complex Wishart distribution by normal vectors [54]. Note that the first order moment of $\mathbf{W} \sim CW_M\left(N, \Sigma, \Sigma^{-1}\mathbf{M}\mathbf{M}^H\right)$ and of the approximation $\mathbf{W}'$ are identical, whereas the second order moment differs by $\frac{1}{N}\mathbf{M}^H\mathbf{M}$. Hence, this justifies the approximation. In this case the probability density function (PDF) of the post-processing SNR of each stream is given by [21]

$$f(\gamma_k) = \frac{\left([\Sigma']_{kk}^{-1}\right) e^{-\left(\frac{\gamma_k}{\gamma_0}\right)[\Sigma']_{kk}^{-1}}}{\gamma_0 \Gamma(N - M + 1)} \left(\left(\frac{\gamma_k}{\gamma_0}\right)[\Sigma']_{kk}^{-1}\right)^{N-M}, \tag{3.11}$$

with $k = 1, 2, \ldots, M$, Γ denotes the Gamma function, and $[\Sigma']_{kk}^{-1}$ is the (k,k)th element of the matrix $[\Sigma']^{-1}$.

From (3.11), one can see that in order to determine all the parameters of the central chi-square PDF of γ_k, we have to determine $[\Sigma']_{kk}^{-1}$. Now the covariance matrix, denoted by Σ', can be written as

$$\Sigma' = \frac{1}{\kappa+1}\mathbf{R}_t + \frac{\kappa}{\kappa+1}\left(\frac{1}{N}\right)\left(Ne^{j\frac{\pi}{4}}\right)\Psi_{M,M}.$$ (3.12)

Using the definition of matrix inversion, we have

$$[\Sigma']_{kk}^{-1} = \frac{\det\left[\Sigma'_{kk}\right]}{\det(\Sigma')},$$ (3.13)

where $\det(\cdot)$ denotes the determinant of matrices and $\det[\Sigma'_{kk}]$ is the minor determinant of the matrix Σ'. Inspection of (3.13) reveals that in order to obtain a closed-form expression for the BER of each substream, we have to transform the matrix in (3.12) into a lower or upper diagonal matrix. To do this, we let $\xi = \frac{\kappa}{\kappa+1}$ and then we perform row manipulation on the matrix to get

$$\Sigma' = \begin{bmatrix} (1-\xi)(1-|\rho|^2)(1-\rho^*) & (1-\xi)(|\rho|^2-1) & 0 & \dots 0 \\ \rho^*(1-|\rho|^2)(1-\rho^*) & (1-\xi)(1-|\rho|^2)(1-\rho^*) & (1-\xi)(|\rho|^2-1) & \dots 0 \\ \rho^{*2}(1-|\rho|^2)(1-\rho^*) & \rho^*(1-\xi)(1-|\rho|^2)(1-\rho^*) & (1-\xi)(1-|\rho|^2)(1-\rho^*) & \dots(1-\xi)(|\rho|^2-1) \\ \vdots & \vdots & \vdots & \vdots \\ \rho^{*(t-1)}(1-\xi)+\xi e^{j\frac{\pi}{4}} & \rho^{*(t-2)}(1-\xi)+\xi e^{j\frac{\pi}{4}} & \rho^{*(t-3)}(1-\xi)+\xi e^{j\frac{\pi}{4}} & \dots(1-\xi)+\xi e^{j\frac{\pi}{4}} \end{bmatrix}.$$ (3.14)

We noted that one cannot reduce this matrix to lower or upper diagonal. Thus, we let

$$[\Sigma']_{kk}^{-1} = \frac{\det\left[\Sigma'_{kk}\right]}{\det(\Sigma')} = \frac{\beta}{\alpha},$$ (3.15)

where β and α are the minor determinant and the determinant of matrix Σ' introduced in (3.14), respectively. It is essential to keep in mind that (3.14) is used to evaluate β and α numerically.

Next we use (3.15) to determine the parameters of the central chi-square distribution

30

given in [12,21]

$$f(\gamma_k) = \frac{\left(\frac{\beta}{\alpha\gamma_0}\right)}{\Gamma(N-M+1)} e^{-\left(\frac{\beta}{\alpha\gamma_0}\right)\gamma_k} \left(\left(\frac{\beta}{\alpha\gamma_0}\right)\gamma_k\right)^{N-M}, \qquad (3.16)$$

with $k = 1, 2, \ldots, M$.

The average BER of each substream can then be obtained by averaging the instantaneous BER $P(\gamma_k)$ over all SNRs [5], i.e.,

$$P_k = \int_0^{+\infty} P(\gamma_k) f(\gamma_k) d\gamma_k. \qquad (3.17)$$

For QPSK modulation, the average BER can be expressed as

$$P_k = \frac{\left(\frac{\beta}{\alpha\gamma_0}\right)^{(N-M+1)}}{\Gamma(N-M+1)} \int_0^{+\infty} e^{-\left(\frac{\beta}{\alpha\gamma_0}\right)} (\gamma_k)^{N-M} Q\left(\sqrt{2\gamma_k}\right) d\gamma_k, \qquad (3.18)$$

where $Q(\cdot)$ is the complementary error function. Using [Eq. (A1) in [55]] with $a = \left(\frac{\beta}{\alpha\gamma_0}\right)$, $t = \gamma_k$, $b = (N-M+1)$, $c = 2$, the average BER is given by [56]

$$P_k = \frac{1}{2}\left[1 - \tau \sum_{i=0}^{N-M} \binom{2i}{i} \left(\frac{1-\tau^2}{4}\right)^i\right], \qquad (3.19)$$

with $\tau = \sqrt{\frac{\alpha\gamma_0}{\beta+\alpha\gamma_0}}$.

Recall that the diversity order of a system is given by [10]

$$D = -\lim_{\gamma_0 \to \infty} \frac{\log P_k(\gamma_0)}{\log(\gamma_0)}. \qquad (3.20)$$

Using (3.20), and applying L'Hôpital's rule, one can show that the diversity gain is $D = N - M + 1$. Thus, the diversity gain of the system agrees with the result in [12]. Note that, in our analysis, we assume that the channel matrix $\mathbf{H}$ contains transmit antenna correlation

31

but no receive antenna correlation. Later, we will investigate the system performance over receive correlated Ricean flat-fading channels. With receive antenna correlation (but no transmit antenna correlation) the channel matrix $\mathbf{H}$ is given by

$$\mathbf{H} = \sqrt{\frac{\kappa}{\kappa+1}}\, e^{j\theta}\, \Psi_{N,M} + \sqrt{\frac{1}{\kappa+1}}\, \mathbf{R}_r^{1/2}\, \mathbf{H}_w, \tag{3.21}$$

where $\mathbf{R}_r$ denotes the $N \times N$ receive covariance matrix and $\mathbf{H}_w$ is an $N \times M$ matrix whose elements are i.i.d. complex Gaussian random variables with zero-mean and unit-variance. We also consider the exponential correlation model, where the entries of $\mathbf{R}_r$ are given by

$$[\mathbf{R}_r]_{i,j} = \begin{cases} r_{Rx}^{j-i}, & i \le j \\ \\ [\mathbf{R}_r]^*_{j,i}, & i > j \end{cases} \quad, \quad |r_{Rx}| \le 1, \tag{3.22}$$

where r_{Rx} is the complex correlation coefficient of neighboring receive branches. In this case, it will be shown that the performance, when $N = M$, is the same as that of transmit correlated Ricean flat-fading channels. However, when $N > M$ the performance is no longer the same.

3.3.2 Optimal Transmit Correlation for TITO-SM Systems

In this section, we derive a closed-form expression for the optimal transmit correlation coefficient which achieves the maximum capacity (i.e., uncorrelated case) of TITO-SM systems over transmit correlated Ricean flat-fading channels. Hence, for any channel realization, we find the optimal $\mathbf{R}_t$ that achieves the maximum capacity. It is essential to keep in mind the fact that channel correlation, which degrades the system capacity, depends on the physical parameters of the MIMO system and the scattering characteristics. These physical parameters include the antenna arrangement and spacing, angle spread, and the transmitted

signal wavelength [20, 48].

Given a transmit correlated Ricean channel matrix $\mathbf{H}$, one can derive an expression for the optimal transmit correlation matrix $\mathbf{R}_t$ in terms of the entries of $\mathbf{H}$ that maximizes the MIMO capacity. Now, the instantaneous capacity expression of a MIMO fading channel is given by [2]

$$\mathbb{C} = \log_2 \det \left[\mathbf{I}_N + \frac{\zeta}{M} \mathbf{H} \mathbf{R}_t \mathbf{H}^H \right], \quad \text{bits/s/Hz}. \tag{3.23}$$

For a $(M = 2, N = 2)$ system, using the exponential correlation model we have

$$\mathbf{R}_t = \begin{bmatrix} 1 & \rho \\ \rho^* & 1 \end{bmatrix}. \tag{3.24}$$

Substituting (3.24) in (3.23), and after differentiation and simplification, the optimal correlation is given by

$$\rho_{opt} = \frac{2}{\zeta} \left(\frac{\phi}{\omega - \sigma} \right), \tag{3.25}$$

where $\phi = (h_{2,1}h_{2,2}^* + h_{1,1}h_{1,2}^*)$, $\omega = (h_{1,2}h_{1,1}^* h_{2,1}h_{2,2}^* + h_{1,1}h_{1,2}^* h_{2,2}h_{2,1}^*)$ and $\sigma = (|h_{2,1}|^2|h_{1,1}|^2 + |h_{2,1}|^2|h_{1,2}|^2)$.

This correlation value will be shown to achieve the optimal Ricean capacity of TITO-SM systems (i.e., uncorrelated case). It is essential to mention that, based on (3.25) and using a feedback information channel to provide the transmitter with full CSI, if practically possible, one can adjust the physical parameters of TITO-SM systems to achieve the maximum capacity (i.e., uncorrelated case). This can be tractable due to the slow fading assumption. Also one can employ adaptive precoding techniques to adjust the transmit correlation to achieve the optimal capacity. As a result, a significant capacity is achieved by exploiting the knowledge of the Ricean channel.

3.4 Simulation Results

In this section, we provide simulations to show the accuracy of our analytical results. In what follows, unless otherwise stated, the performance is measured in terms of BER versus SNR for a frame of 100 vector symbols averaged over 10,000 frames. The channel is modeled as a quasi-static fading with fading coefficients fixed for the duration of the frame and change independently from one frame to another.
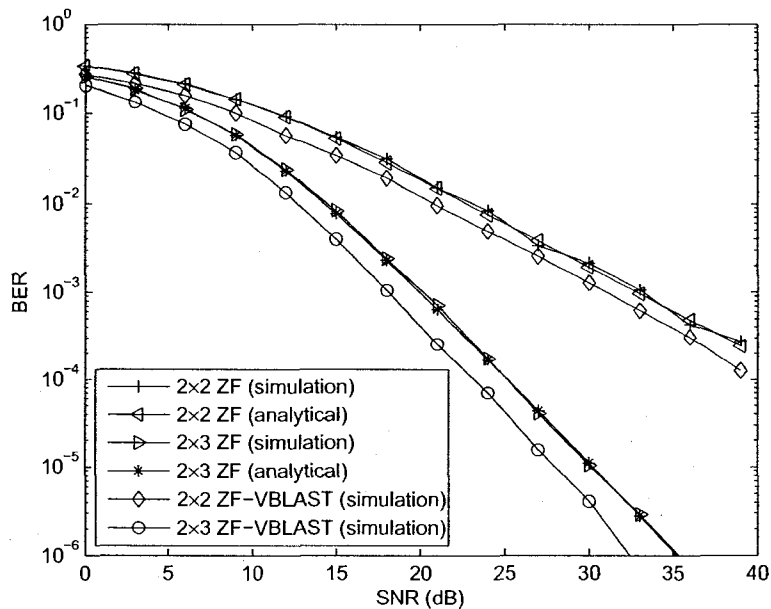
Figure 3.2: BER of ZF detector for $M = 2$ transmit and $N = 2, 3$ receive antennas. QPSK constellations, transmit correlation $|\rho| = 0.8$ and Ricean factor $\kappa = 6$ dB.

In Fig. 3.2 we simulated $(M = 2, N = 2, 3)$ MIMO systems employing ZF receiver along with the approximated BER in (3.19). Note that the analytical and simulated results are in excellent agreement. It can also be seen from Fig. 3.2 that the zero-forcing VBLAST (ZF-VBLAST) receiver [15–17], with optimal ordering detection, reduces the effect of correlation to some extent, but the diversity order remains the same as the ZF linear receiver. Thus (3.19) can serve as an upper bound for the average BER of the ZF-VBLAST receiver

in transmit correlated Ricean flat-fading channels.
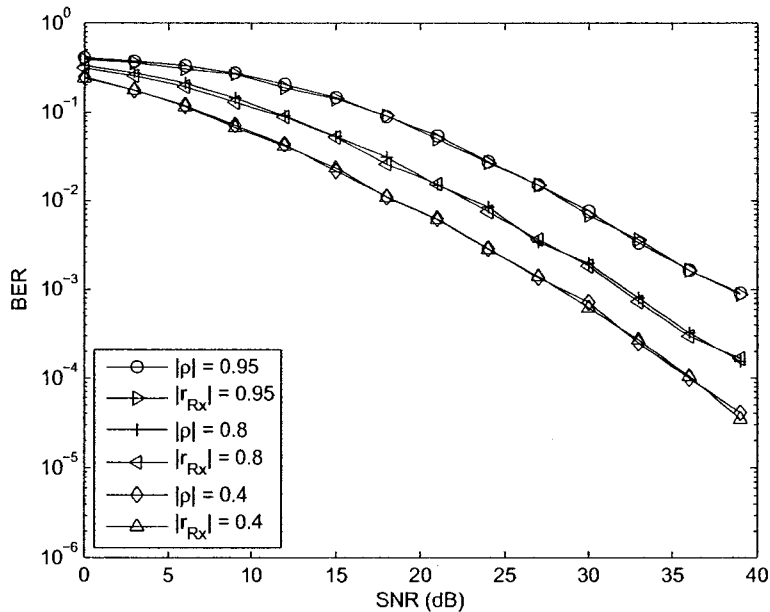
Figure 3.3: BER comparison of ZF detector for $M = 2$, $N = 2$ MIMO system in the case of transmit correlation $|\rho|$ and receive correlation $|r_{Rx}|$, respectively. QPSK constellations, Ricean factor $\kappa = 6$ dB.

In Fig. 3.3, we examine the BER performance of the ZF receiver over transmit and receive correlated flat Ricean fading channels. We consider three correlation settings: *i)* $|\rho| = 0.4$, $|r_{Rx}| = 0.4$; *ii)* $|\rho| = 0.8$, $|r_{Rx}| = 0.8$; *ii)* $|\rho| = 0.95$, $|r_{Rx}| = 0.95$. The results are shown for an $(M = 2, N = 2)$ system. It is clear that, when $N = M$, the BER performance is the same in both cases. This is due to the fact that both covariance matrices are equal. However it can be shown that when $N > M$, the BER performance is no longer the same which is due to the unequal transmit and receive covariance matrices.

Fig. 3.4 depicts the performance of a $(M = 2, N = 2)$ system over transmit correlated Ricean flat-fading MIMO channels for Ricean factor $\kappa = 6$ dB. These performance results are reported in terms of the Ricean capacity versus SNR. We use the ergodic capacity as a metric for performance evaluation, which is obtained by averaging over 2000 independent
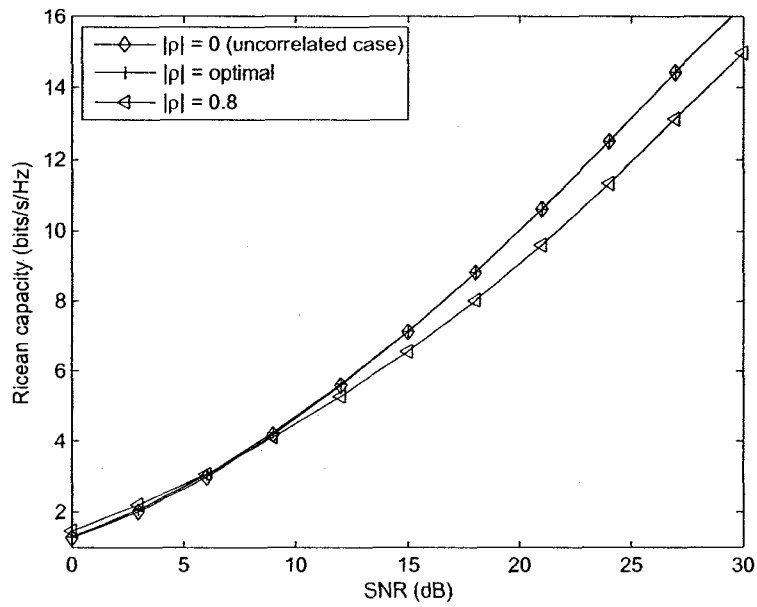
Figure 3.4: Comparison of empirical and analytical Ricean capacity for $M = 2$, $N = 2$ MIMO system. QPSK constellations, transmit correlation $|\rho| = 0$, optimal, 0.8 and Ricean factor $\kappa = 6$ dB.

36

realizations of the channel matrix **H**. We consider three correlation settings: *i*) $|\rho| = 0$ (uncorrelated case); *ii*) $|\rho| =$ optimal, as defined in (3.25); *iii*) $|\rho| = 0.8$. It can be noticed that the performance of the optimal transmit correlated system (i.e., $|\rho| =$ optimal as in (3.25)) perfectly agrees with the case of uncorrelated case ($|\rho| = 0$).
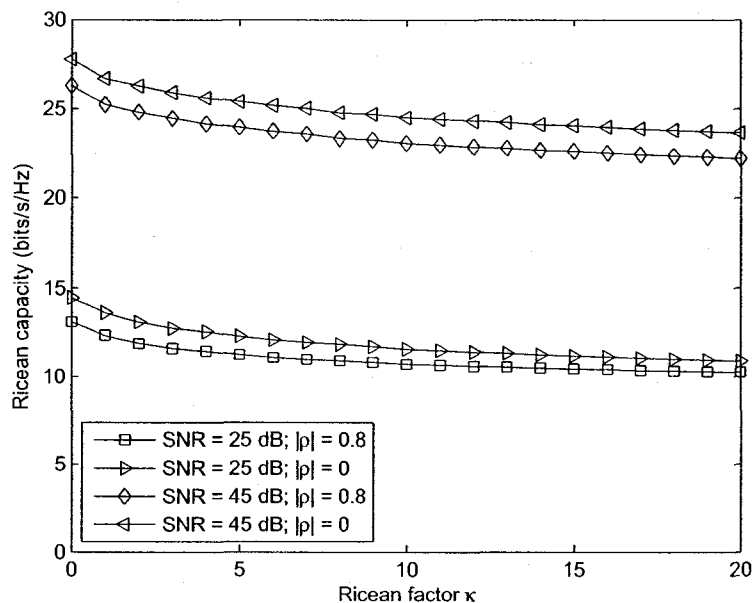
Figure 3.5: Relation between Ricean capacity and Ricean factor κ for $M = 2, N = 2$ MIMO system. Transmit correlation $|\rho| = 0, 0.8$.

Fig. 3.5 shows the relationship between the Ricean capacity and the Ricean factor κ for an $(M = 2, N = 2)$ system. As in Fig. 3.3, we use the ergodic capacity as a metric for performance evaluation, which is obtained by averaging over 2000 independent realizations of the channel matrix **H**. It can be concluded that the Ricean capacity decreases as κ increases.

Finally in Fig. 3.6, we simulate the BER performance of an $(M = 2, N = 2)$ system in transmit correlated flat Ricean fading channels with ZF decoding. We consider the same correlation settings as in Fig. 3.4. It is clearly apparent that the BER performance for the
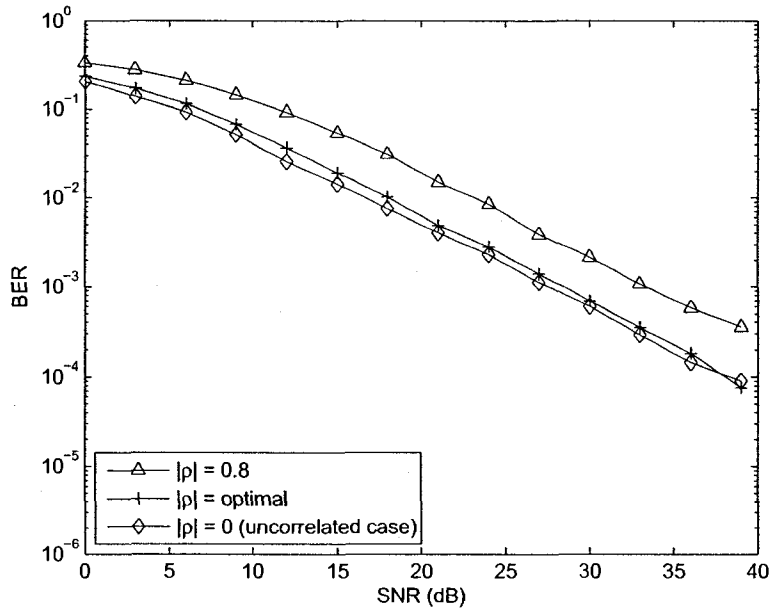
Figure 3.6: BER comparison of ZF detector for $M = 2$, $N = 2$ MIMO system. QPSK constellations, transmit correlation $|\rho| = 0$, optimal, 0.8 and Ricean factor $\kappa = 6$ dB.

optimal transmit correlation value ($|\rho| =$ optimal), defined in (3.25), is very close to the optimal uncorrelated case ($|\rho| = 0$).

3.5 Conclusions

In this chapter, we have analyzed the BER performance of the ZF receiver in transmit correlated Ricean flat-fading channels. In particular, we have derived a near exact approximation for the average BER. Moreover, we have investigated the system performance in receive correlated Ricean flat-fading channels. In that, we have showed that the performance, when $N = M$, is the same as that of transmit correlated Ricean flat-fading channels. In addition, we have derived a closed-form expression for the optimal transmit correlation coefficient, of $\mathbf{R}_t$, which achieves the maximum capacity (i.e., uncorrelated case) of TITO-SM systems. As a result, a significant capacity, without the use of any special signal processing

38

algorithm and/or space-time coding at the receiver, is achieved by exploiting the knowledge

of the Ricean channel.

Chapter 4

Transmit Antenna Selection for DFD in Uncorrelated Rayleigh MIMO Channels

4.1 Introduction

In Chapter 3, we have demonstrated that the DFD outperforms the ZF receiver. We only consider DFD in this chapter. However, the performance enhancement of such receiver comes at the expense of a higher implementation complexity. To this end, we introduce a new pragmatic AS approach that achieves optimal performance with reduced cost of hardware requirements.

4.1.1 Prior Work

AS in spatial multiplexing systems has been addressed in [11, 23–25, 57–60]. Based on argument that it increases capacity, AS for spatial multiplexing was first presented in [23]. More specifically, the authors show that feeding back an optimal subset of transmit antennas often increases system capacity over the case of no feedback. In [24], the authors present suboptimal schemes for receive AS that offer a performance comparable to optimal

capacity-based selection based on exhaustive search [23], but with lower complexity. In that, the authors show that the diversity order achievable through receive AS is the same as that of the full system, which motivates the use of receive AS in spatial multiplexing systems. It is worth highlighting that in [23, 24, 58, 60] AS is studied from the capacity maximization standpoint. Whereas in [11, 25, 57, 59] AS is investigated from the perspective of error probability, where the authors propose AS algorithms that aim to minimize the BER of linear receivers. For instance, transmit AS for spatial multiplexing when the ZF receiver is used, is presented in [25, 57, 59]. A transmit multimode AS, which improves the error rate performance of spatial multiplexing systems with linear receivers, is presented in [11]. In the multimode AS, both the number of substreams and the mapping from substreams to antennas are optimally chosen based on the channel. For a review of various transmit and receive AS schemes, the interested reader is referred to [18, 19].

4.1.2 Contributions and Organization

In this chapter, we investigate the performance of a transmit AS scheme for the DFD over independent Rayleigh distributed flat-fading channels. We first present the system model in Section 4.2. In Section 4.3, we present a pragmatic AS criterion that maximizes both the post-processing SNR at the receiver, and the system capacity. Specifically, we propose a reduced complexity scheme that selects the optimal K antennas out of the M available ones. Compared to the use of all antennas, this has the advantage that only $K (K < M)$ instead of M transmit analog RF chains are required. Note that we still need the full number of M antenna elements (patch or dipole), but these are generally cheaper elements. Analysis on the outage probability for the AS approach is presented in Section 4.4. Simulation results are provided in Section 4.5 to validate and demonstrate the performance. Finally, conclusions are given in Section 4.6.

41
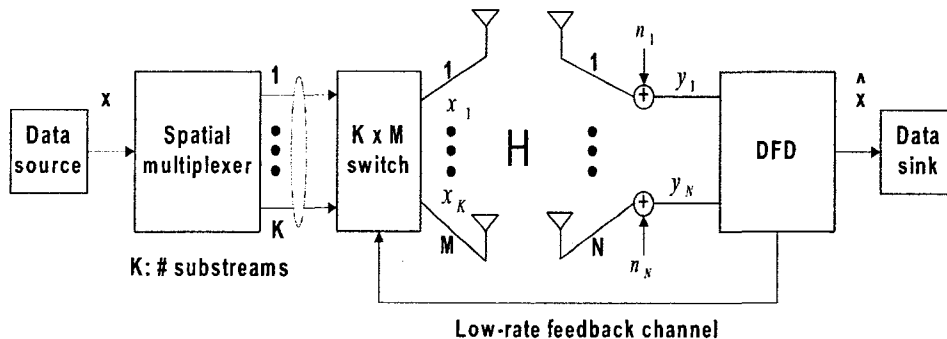
Figure 4.1: MIMO-SM system employing DFD and performing transmit AS.

4.2 System Model

Consider a point-to-point single-user MIMO-SM system that employs M transmit and $N (N \geq M)$ receive antennas, and a $1 : K (K < M)$ spatial multiplexer as shown in Fig. 4.1. The system works as follows. At one symbol time, K input symbols are multiplexed to produce the K-dimensional symbol vector x for transmission over K active transmit antennas out of M possible ones. The optimal subset p, which constitutes of the K transmit antennas, is determined by a selection algorithm operating at the receiver. The latter indicates, at each fading state, to the transmitter through a low-bandwidth, zero-delay and error-free feedback channel, the optimal subset $p \in P$ of size K. Note that P is the set of all possible subsets of selected transmit antennas given by

$$P = \left\{ \binom{M}{K}; \text{ for a given } K (K < M) \right\}. \tag{4.1}$$

Then the data vector x is sent through the channel, which is assumed to be flat-fading and slowly-time varying. At the receiver side, antennas receive the K substreams which are mixed and superimposed by noise. Now it is the role of the DFD to detect and separate the substreams one-by-one.

Let **H** denote the $N \times M$ channel matrix, and $\mathbf{H}_p$ denote the $N \times K$ channel submatrix

42

corresponding to the selected transmit antennas in p. The corresponding sampled received baseband signal is given by

$$\mathbf{y} = \mathbf{H}_p \mathbf{E}_p \mathbf{x} + \mathbf{n}, \qquad (4.2)$$

where $\mathbf{y} \in C^{N \times 1}$ is the received signal, $\mathbf{E}_p \in \mathbb{R}^{K \times K}$ is a channel-dependent permutation matrix corresponding to the detection ordering. $\mathbf{H}_p \in C^{N \times K}$ consists of i.i.d. circularly symmetric Gaussian random variables with zero-mean and unit-variance, i.e., $h_{i,j} \sim CN(0,1)$ for $1 \le i \le N$, $1 \le j \le K$. We assume that the fading coefficients are constant over the entire frame and vary independently from one frame to another (quasi-static fading). We assume that the receiver has a perfect knowledge of the channel matrix $\mathbf{H}$. The information symbol vector $\mathbf{x} \in C^{K \times 1}$ consists of independent and uniform power transmitted substreams. The receiver noise $\mathbf{n} \sim CN(0, N_0 \mathbf{I}_N)$ consists of independent circularly symmetric zero-mean complex Gaussian entries of variance N_0.

4.3 Proposed Transmit Antenna Selection Approach

The DFD algorithm [14], which is also known in the MIMO literature as VBLAST [15–17], was shown to suppress the interference by either ZF or MMSE criterion. However, here we constrain our discussion to the ZF case. The reason is that the ZF nulling criterion has low implementation complexity and makes our analysis more tractable than that of MMSE. Furthermore, the ZF receiver performance approaches that of MMSE at high-SNR. Since no selection is performed yet, in this section we use the full channel matrix $\mathbf{H}$. It is well-known that the DFD can be concisely represented by the QR decomposition [42,61], i.e., $\mathbf{H} = \mathbf{QR}$, where $\mathbf{Q}$ is an $N \times M$ semi-unitary matrix $\left(\mathbf{Q}^H \mathbf{Q} = \mathbf{I}_M\right)$ with its orthonormal columns being the ZF nulling vectors, and $\mathbf{R}$ is an $M \times M$ upper triangular matrix with real-valued positive diagonal entries. Correspondingly, the ordered DFD can be represented by applying the QR decomposition to $\mathbf{H}$ with its columns permuted, i.e., $\mathbf{HE} = \mathbf{QR}$, where

E is the full channel-dependent permutation matrix (i.e., function of **H**). The receiver performs a QR factorization of **H**, and then it implements two operations: nulling and cancellation.

Since no selection is yet performed, we have

$$\mathbf{y} = \mathbf{QRx} + \mathbf{n}. \tag{4.3}$$

The transmitted symbols are detected as follows. Multiplying both sides of (4.3) by $\mathbf{Q}^H$ yields

$$\tilde{\mathbf{y}} = \mathbf{Rx} + \tilde{\mathbf{n}}, \tag{4.4}$$

where $\tilde{\mathbf{n}} = \mathbf{Q}^H \mathbf{n}$ and $\tilde{\mathbf{y}} = \mathbf{Q}^H \mathbf{y}$. It is worth noting that the nulling operation (i.e., $\mathbf{Q}^H \mathbf{y}$) is a coordinate rotation which produces an M-dimensional vector $\tilde{\mathbf{y}}$ that constitutes a sufficient statistic. The aim of the nulling operation is to render **H** in upper triangular matrix, but with no amplification of the receiver noise (**Q** is unitary). Therefore, $\tilde{\mathbf{n}}$ is still $\sim CN(0, N_0 \mathbf{I}_N)$. Now one could multiply by $\mathbf{R}^{-1}$ which would be the typical ZF nulling technique, but significant improvements can be obtained through SIC.

The received vector $\tilde{\mathbf{y}}$, in matrix form, can be written as

$$
\begin{bmatrix} \tilde{y}_1 \\ \tilde{y}_2 \\ \vdots \\ \tilde{y}_M \end{bmatrix} = \begin{bmatrix} r_{1,1} & r_{1,2} & \cdots & r_{1,M} \\ 0 & r_{2,2} & \cdots & r_{2,M} \\ \vdots & \ddots & \ddots & \vdots \\ 0 & \cdots & 0 & r_{M,M} \end{bmatrix} \begin{bmatrix} x_1 \\ x_2 \\ \vdots \\ x_M \end{bmatrix} + \begin{bmatrix} \tilde{n}_1 \\ \tilde{n}_2 \\ \vdots \\ \tilde{n}_M \end{bmatrix}. \tag{4.5}
$$

The general sequential signal detection, which involves cancellation (decision feedback), is given by

$$\hat{x}_i = C \left[\frac{1}{r_{i,i}} \left(\tilde{y}_i - \sum_{j=i+1}^{M} r_{i,j} \hat{x}_j \right) \right], \quad \text{for} \quad i = M, M-1, \ldots, 1, \tag{4.6}$$

44

where $r_{i,i}$ and $r_{i,j}$ are the (i,i)th and (i,j)th entries of $\mathbf{R}$, respectively. Inspection of (4.5) reveals that, to estimate x_M, the receiver needs to multiply by the inverse of $r_{M,M}$. Thus $\tilde{y}_M$ constitutes a virtual subchannel that has no interference from other subchannels. Hence, the decision statistic for the Mth received symbol is

$$
\begin{aligned}
\hat{x}_M &= C\left[\left(\frac{1}{r_{M,M}}\right)\tilde{y}_M\right] \\
&= C\left[x_M + \left(\frac{1}{r_{M,M}}\right)\tilde{n}_M\right].
\end{aligned}
\tag{4.7}
$$

However, $\tilde{y}_{M-1}$ is subject to interference from the Mth subchannel through the off-diagonal entry $r_{M-1,M}$. Using (4.6), the decision statistic for x_{M-1} is

$$
\begin{aligned}
\hat{x}_{M-1} &= C\left[\frac{1}{r_{M-1,M-1}}\left(\tilde{y}_{M-1} - r_{M-1,M}\hat{x}_M\right)\right] \\
&= C\left[\frac{1}{r_{M-1,M-1}}\left(r_{M-1,M-1}x_{M-1} + n_{M-1} + r_{M-1,M}\left(x_M - \hat{x}_M\right)\right)\right].
\end{aligned}
\tag{4.8}
$$

If the detection of x_M is correct, we can get a correct estimate of x_{M-1} with a high probability, and so on. Assume that the previous decisions are correct (i.e., no propagation of error), the DFD decouples the MIMO channel into a set of M independent, parallel SISO virtual subchannels, and the different substreams can be expressed as

$$
\tilde{y}_i = r_{i,i}x_i + \tilde{n}_i, \quad \text{for} \quad i = 1, 2, \ldots, M.
\tag{4.9}
$$

Since $\mathbb{E}\left[\tilde{n}\,\tilde{n}^H\right] = N_0\mathbf{I}_N$, the output SNR of the ith substream is given by

$$
\gamma_i = r_{i,i}^2\gamma_0,
\tag{4.10}
$$

where $\gamma_0 = \zeta/M$ is the average normalized received SNR at each receive antenna. Thus, the output SNRs of the substreams are determined by the diagonal entries of the matrix $\mathbf{R}$

which in turn depend on **E**. Based on (4.10), a pragmatic AS criterion would be to choose the subset of antennas with the highest $r_{i,i}$'s values. Now, it is essential to mention that our AS criterion is also applicable to the case where propagation of error exists. In this case, one can show that the general sequential decision statistic can be written as

$$\hat{x}_{M-i} = C \left[x_{M-i} + \frac{1}{r_{M-i,M-i}} \left(\tilde{n}_{M-i} + \sum_{j=M-i+1}^{M} r_{M-i,j} \Delta e_j \right) \right], \qquad (4.11)$$

with $0 \leq i \leq M - 1$, and Δe_j denotes the error term resulting from the hard/soft estimate made on the x_j symbol. Hence to minimize the error term, we have to select the largest $r_{i,i}$'s values. The reason is that the error term is inversely proportional to $r_{i,i}$'s values.

Now, it is important to mention that the proposed transmit AS criterion maximizes the system capacity. Using (4.10), we can see that the channel capacity is now equivalent to the capacity of a MIMO-SM system with linear receiver employed, since we have neglected the propagation of error. Thereby the channel is now decoupled into M parallel substreams, for which the capacity is given by [12]

$$\mathbb{C} = \sum_{i=1}^{M} \log_2 (1 + \gamma_i), \qquad (4.12)$$

where γ_i is the post-processing SNR for the ith substream. Now substituting (4.10) in (4.12), we have

$$\mathbb{C} = \sum_{i=1}^{M} \log_2 \left(1 + r_{i,i}^2 \gamma_0 \right). \qquad (4.13)$$

Clearly, the adopted selection criterion is optimal in the sense that it maximizes both the post-processing SNR at the receiver side, and the system capacity. It can be shown that when $M = N$ the proposed AS algorithm has a complexity of $O\left(M^3\right)$, whereas the selection algorithm proposed in [23] has a complexity of $O\left(M^5\right)$.

46

4.4 Outage Probability Analysis

In this section, we present a comprehensive analysis of the outage probability for the AS scheme over independent Rayleigh fading channels. An upper bound on the outage probability at high-SNR regime is presented.

Recall that the instantaneous capacity expression of a MIMO fading channel (without performing AS) is given by [2]

$$\mathbb{C} = \log_2 \det \left[\mathbf{I}_M + \frac{\zeta}{M} \mathbf{H}^H \mathbf{H} \right], \quad \text{bits/s/Hz.} \tag{4.14}$$

Now, an outage event occurs when the information transmission rate, denoted by $\mathcal{R}$, is greater than the instantaneous capacity $\mathbb{C}$. Hence, the outage probability is given by [3]

$$\mathcal{P}_{\text{outage}} = \Pr(\mathbb{C} < \mathcal{R}). \tag{4.15}$$

To derive an upper bound on the outage probability, we have to consider the case of single selected transmit antenna. According to our approach, this single selected transmit antenna, denoted by v, is determined by

$$v = \arg\max_{1 \leq i \leq M} \left\{ r_{i,i}^2 \right\}. \tag{4.16}$$

The upper bound on the outage probability for the AS scheme can then be written as

$$
\begin{aligned}
\mathcal{P}_{\text{outage,AS}} &\leq \Pr\left\{ \log_2\left(1 + r_{v,v}^2 \frac{\zeta}{M} \right) < \mathcal{R} \right\} \\
&\leq \Pr\left\{ r_{v,v}^2 < \frac{(2^{\mathcal{R}} - 1) M}{\zeta} \right\} \\
&\leq \mathcal{F}_{r_{v,v}^2}\left(\frac{(2^{\mathcal{R}} - 1) M}{\zeta} \right),
\end{aligned} \tag{4.17}
$$

where $\mathcal{F}_{r_{v,v}^2}(\cdot)$ is the cumulative distribution function (CDF) of the random variable $r_{v,v}^2$. Also, using the fact that $r_{v,v}^2$ is the largest order statistic [62], the CDF of $r_{v,v}^2$ can be written as

$$\mathcal{F}_{r_{v,v}^2}\left(\frac{\left(2^{\mathcal{R}}-1\right)M}{\zeta}\right) = \mathcal{F}_{r_{1,1}^2}\left(\frac{\left(2^{\mathcal{R}}-1\right)M}{\zeta}\right) \times \ldots \times \mathcal{F}_{r_{M,M}^2}\left(\frac{\left(2^{\mathcal{R}}-1\right)M}{\zeta}\right). \quad (4.18)$$

Now substituting (4.18) in (4.17), we get

$$\mathcal{P}_{\text{outage,AS}} \leq \mathcal{F}_{r_{1,1}^2}\left(\frac{\left(2^{\mathcal{R}}-1\right)M}{\zeta}\right) \times \ldots \times \mathcal{F}_{r_{M,M}^2}\left(\frac{\left(2^{\mathcal{R}}-1\right)M}{\zeta}\right). \quad (4.19)$$

It is important to keep in mind the fact that the entries of $\mathbf{R}$ are independent of each other. Moreover, with fixed $\mathbf{E}$, the square of the ith diagonal element of $\mathbf{R}$, $r_{i,i}^2$, is of central chi-square distribution with $2(N-i+1)$ degrees of freedom [53, 63], i.e., $r_{i,i}^2 \sim \chi^2_{2(N-i+1)}$. Consequently, $\mathcal{F}_{r_{i,i}^2}\left(\frac{\left(2^{\mathcal{R}}-1\right)M}{\zeta}\right)$ with $1 \leq i \leq M$, is the CDF of a central chi-square distribution $\sim \chi^2_{2(N-i+1)}$. Using this fact, the CDF can be expressed as [64]

$$\mathcal{F}(x,k) = P\left(\frac{k}{2},\frac{x}{2}\right), \quad (4.20)$$

where $P(k,x)$ denotes a normalized incomplete Gamma function (regularized Gamma function) defined as [64]

$$P(k,x) = \frac{1}{\Gamma(k)}\int_0^x e^{-t}t^{k-1}\,dt,$$

where $k\,(k \geq 0)$ denotes the degrees of freedom.

Now substituting (4.20) in (4.19), we get

$$\mathcal{P}_{\text{outage,AS}} \leq \left[P\left(N,\frac{\left(2^{\mathcal{R}}-1\right)M}{2\zeta}\right)\right] \times \ldots \times \left[P\left(N-M+1,\frac{\left(2^{\mathcal{R}}-1\right)M}{2\zeta}\right)\right]. \quad (4.21)$$

48

The power series expansion of $P(k,x)$ is given by [64]

$$
\begin{aligned}
P(k,x) &= x^k \gamma^*(k,x) \\
&= x^k e^{-x} \sum_{n=0}^{\infty} \frac{x^n}{\Gamma(k+n+1)},
\end{aligned}
\tag{4.22}
$$

where $\gamma^*(k,x)$ is the incomplete Gamma function. In order to get $\mathcal{P}_{\text{outage,AS}}$ at high-SNR, we substitute (4.22) in (4.21). Now, using the fact that $\Gamma(z) = (z-1)!$, where z is a positive integer, $\mathcal{P}_{\text{outage,AS}}$ at high-SNR can be written as [65]

$$
\begin{aligned}
\mathcal{P}_{\text{outage,AS}} &\leq \left(\frac{(2^{\mathcal{R}}-1) M}{2} \right)^{\sum_{i=1}^{M}(N-i+1)} \left(\frac{1}{\prod_{i=1}^{M}(N-i+1)!} \right) \\
&\quad \times \zeta^{-\sum_{i=1}^{M}(N-i+1)} \\
&\leq \left(\frac{(2^{\mathcal{R}}-1) M}{2} \right)^{-\left(MN-\frac{1}{2}(M^2-M)\right)} \left(\frac{1}{\prod_{i=1}^{M}(N-i+1)!} \right) \\
&\quad \times \zeta^{-\left(MN-\frac{1}{2}(M^2-M)\right)}.
\end{aligned}
\tag{4.23}
$$

It can be readily seen from (4.23) that the diversity order of the outage probability for the AS scheme is lower bounded by

$$
D_{\text{AS}} \geq MN - \frac{1}{2}\left(M^2 - M\right),
\tag{4.24}
$$

which is less than the MN full complexity diversity order, but much more greater than the N diversity order of the $(M=1,N)$ system. Therefore, (4.24) suggests that in order to achieve a diversity order close to the MN full complexity system, it suffices to have $N \geq M$ and keep M small.
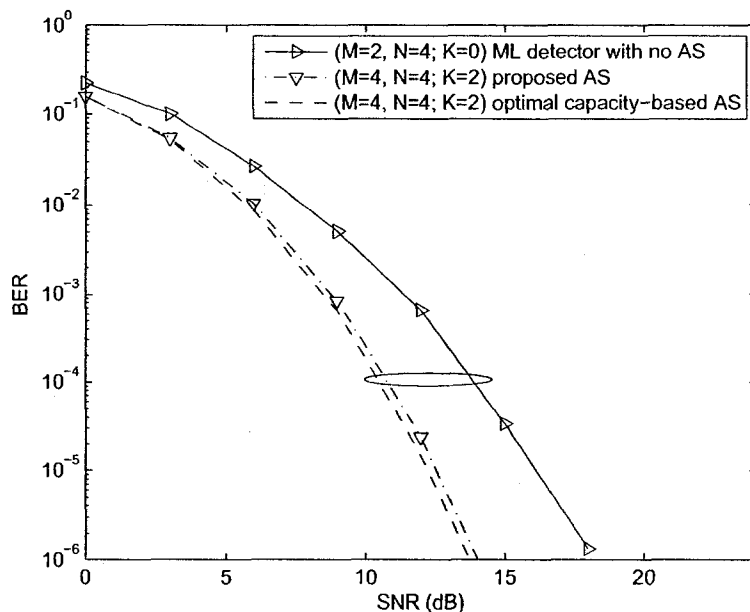
49

Figure 4.2: Comparison of different AS schemes over independent Rayleigh flat-fading channels, and QPSK transmission.

4.5 Simulation Results

In this section, we present both analytical and simulation results for the AS scheme in independent Rayleigh flat-fading channels. In the following, a system with M transmit and N receive antennas out of which K transmit antennas are chosen, is referred to as an $(M,N; K)$ system.

In Fig. 4.2, we evaluate the performance of the proposed transmit AS approach. The performance is measured in terms of the BER for a frame of 100 symbols from QPSK complex constellations averaged over 10,000 frames. As shown, Fig. 4.2 depicts the BER performance of the $(M = 4, N = 4; K = 2)$ system employing DFD and performing the proposed AS scheme. We plot along, as a benchmark, the performance of the same system performing optimal capacity-based AS approach [23]. Also, for reference, we plot along the performance of the $(M = 2, N = 2; K = 0)$ system employing ML detector without

performing AS. It is clear from the figure that the $(M = 2, N = 4; K = 2)$ performing the proposed AS achieves the same performance as the system performing optimal capacity-based AS. It can be noticed that both approaches outperform the $(M = 2, N = 2; K = 0)$ system employing ML detector. Note that here all systems have the same bandwidth efficiency.
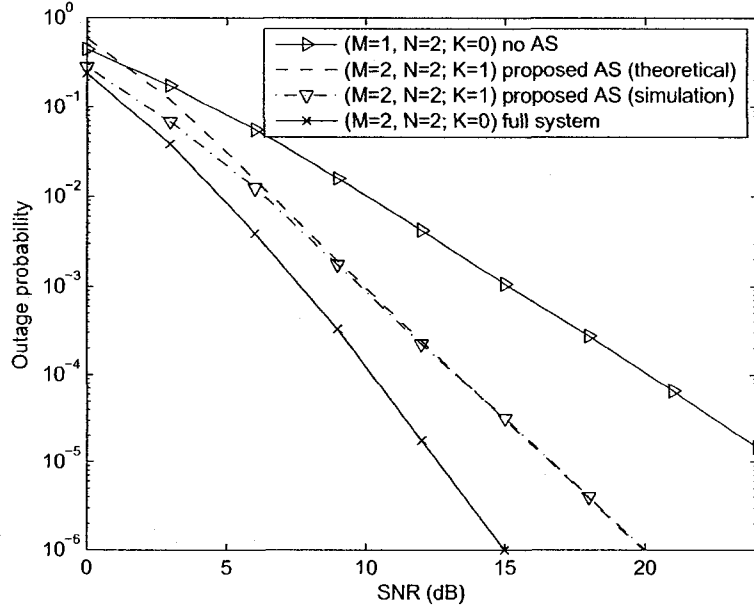
Figure 4.3: Outage probability comparison over independent Rayleigh flat-fading channels. $\mathcal{R} = 2$ bits/s/Hz, and QPSK transmission

Fig. 4.3 displays the outage probability for a $(M = 2, N = 2; K = 1)$ system performing the proposed transmit AS. For the same system, we plot along the closed-form expression given in (4.23). As a benchmark, we plot along the outage probability curves for the $(M = 2, N = 2; K = 0)$ and $(M = 1, N = 2; K = 0)$ systems, respectively. The figure clearly shows that the curves of the closed-form analytical expression in (4.23) and the simulated one are in excellent agreement at high-SNR. As can be observed both curves achieves diversity order of three $(D = 3)$, confirming our analytical results.

4.6 Conclusions

In this chapter, we have analyzed the performance of an AS approach for the DFD receiver over independent Rayleigh flat-fading channels. We used a pragmatic selection criterion that maximizes both the post-processing SNR at the receiver end, and the system capacity. We have derived an upper bound expression on the outage probability for the AS at high-SNR regime. We have also shown that the performance of the proposed AS scheme is comparable to the optimal capacity-based selection based on exhaustive search, but with much less complexity.

Chapter 5

Cross-Layer Based Transmit Antenna Selection for DFD in Correlated Ricean MIMO Channels

5.1 Introduction

In the previous chapter, we have studied AS from a physical layer perspective (e.g., capacity and error probability criteria). In this chapter, we investigate a cross-layer AS approach for MIMO-SM employing DFD at the receiver. The focus on a cross-layer AS scheme can be motivated as follows. In practice, link quality is determined by both physical and data link layers.

5.1.1 Prior Work

A cross-layer approach that combines AS and adaptive modulation, in Rayleigh fading channels, is investigated in [26], in which a H-ARQ technique is used at the data-link layer to improve the link throughput. However, it is important to mention that the authors

in [26] relied on assumptions that are too optimistic to be practical: *i*) uncorrelated signal propagation paths; *ii*) absence of direct-path propagation; *iii*) CSI perfectly known at the receiver. Only more recently, researchers realized the importance of these issues, where measurement results indicate that channels suffer from correlation [27]. The effects of Ricean fading on the capacity of multiple-antenna systems is examined in [28]. In [28], the authors show that Ricean fading can improve the capacity of a multiple-antenna system when the transmitter knows the Ricean factor. MIMO systems with BLAST [4] and orthogonal training signals have been investigated in [29]. In [29], it is shown that one generally spends half of the coherence interval training in order to maximize the throughput in a wireless channel.

5.1.2 Contributions and Organization

In this chapter, we investigate the performance of a cross-layer AS approach. We consider a spatially correlated Ricean fading channel model, which is known to more accurately model real-world wireless environments [22]. An outline of the chapter is as follows. The system model is developed in Section 5.2. The cross-layer AS approach is presented in Section 5.3. In that, a closed-form expression for the system throughput, with perfect CSI at the receiver, is presented. We further analyze the system performance with pilot-channel estimation. Section 5.4 provides a detailed analysis on the extensive simulation results. Finally, conclusions are given in Section 5.5.

5.2 System Model

Consider a point-to-point single-user MIMO wireless packet switched communication system with M transmit and N ($N \geq M$) receive antennas as shown in Fig. 5.1. At the link level a go-back-n (GBN) protocol [66] is adopted. At the receiver end, we have a DFD to
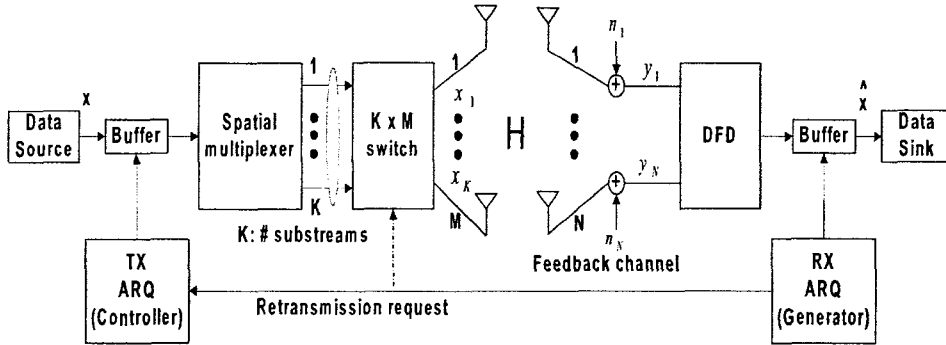
Figure 5.1: MIMO-SM system employing DFD and performing cross-layer based transmit AS.

cancel interference and improve detection of the transmitted packets.

We assume that transmissions are organized in frames, all of fixed predefined length L. For instance, this can be the server information transmitted during client requests. It is worth highlighting that each frame contains a variable number of packets, which is equal to K active antennas out of the M available ones. At the transmitter, the incoming data is fed into a spatial multiplexer that splits the input data streams among the K active antennas out of the M possible ones. The subset of $K \leq M$ transmit antennas is determined by a selection algorithm operating at the receiver, which indicates to the transmitter, through a low-bandwidth, zero-delay and error-free feedback channel, the optimal subset $p \in P'$ of size K. Note that P' is the set of all possible subsets of selected transmit antennas given by

$$P' = \left\{ \binom{M}{K}; \text{ for } K = 1, 2, \ldots, M \right\}. \tag{5.1}$$

Let $\mathbf{H}$ denote the $N \times M$ channel matrix, and $\mathbf{H}_p$ denote the $N \times K$ channel submatrix corresponding to transmit antennas p. Recall that the corresponding sampled received baseband signal is given by

$$\mathbf{y} = \mathbf{H}_p \mathbf{E}_p \mathbf{x} + \mathbf{n}, \tag{5.2}$$

55

where $\mathbf{y} \in C^{N \times 1}$ is the received signal, $\mathbf{E}_p \in \mathbb{R}^{K \times K}$ is a permutation matrix corresponding to the greedy QR detection ordering [67], and $\mathbf{H}_p \in C^{N \times K}$ is the spatially correlated Ricean channel matrix. We assume that the fading process is sufficiently slow to consider it constant for the duration of a frame. The information symbol vector $\mathbf{x} \in C^{K \times 1}$ consists of independent and uniform power transmitted substreams. The receiver noise $\mathbf{n} \sim CN(0, N_0 \mathbf{I}_N)$ consists of independent circularly symmetric zero-mean complex Gaussian entries of variance N_0.

The Ricean channel matrix $\mathbf{H}_p$, that contains transmit and receive antennas correlation, can be written as [45, 68, 69]

$$\mathbf{H}_p = \bar{\mathbf{H}}_{\text{LOS}} + \mathbf{R}_r^{1/2} \bar{\mathbf{H}}_w \mathbf{R}_t^{1/2}, \tag{5.3}$$

where

$$\bar{\mathbf{H}}_{\text{LOS}} = \sqrt{\frac{\kappa}{\kappa+1}} \mathbf{H}_{\text{LOS}} \text{ and } \bar{\mathbf{H}}_w = \sqrt{\frac{1}{\kappa+1}} \mathbf{H}_w.$$

The $N \times N$ matrix $\mathbf{R}_r$ and the $K \times K$ matrix $\mathbf{R}_t$ are the receive and transmit correlation matrices, respectively. Both matrices are assumed to be positive definite, and their elements represent the correlation between antenna pairs at the receiver and transmitter, respectively.

In order to focus on the impact of spatial correlation on the cross-layer transmit AS approach, we assume the receiver to be located at a richly-scattered propagation environment while the transmitter is located at a high altitude. Thereby, the fading is only transmit correlated. This situation can occur, for instance, in indoor environments. Consequently, in this case we have $\mathbf{R}_r = \mathbf{I}_N$ and $\mathbf{R}_t \neq \mathbf{I}_K$, where $\mathbf{I}_K$ is an identity matrix of size K. Note that a frequently used model for $\mathbf{H}_{\text{LOS}}$ is $\mathbf{H}_{\text{LOS}} = \sqrt{\kappa/(\kappa+1)} \, \Psi_{N \times K}$ where $\Psi_{N \times K}$ is an $N \times K$ matrix of all ones [70]. Hence, the channel matrix $\mathbf{H}_p$ can now be written as

$$\mathbf{H}_p = \sqrt{\frac{\kappa}{\kappa+1}} \Psi_{N \times K} + \sqrt{\frac{1}{\kappa+1}} \mathbf{H}_w \mathbf{R}_t^{1/2}. \tag{5.4}$$

56

As in Chapter 3, we constrain our discussion to the exponential correlation model [49,71].

5.3 Adaptive Cross-layer Based Transmit Antenna Selection Approach

In this section, we present a detailed analysis on the throughput performance of the cross-layer AS approach. In that, a closed-form expression of the system throughput is derived under the assumption of perfect CSI at the receiver. Next, we obtain a closed-form expression of the system throughput with imperfect channel estimation.

In the subsequent analysis we constrain our discussion to $\mathbf{H}_p$, which consists of the appropriate columns of $\mathbf{H}$ as dictated by the optimal subset p. Note that, in [23,25], the selected transmit antennas are those that maximize the system capacity according to

$$\mathbb{C}\left(\mathbf{H}_p\right) = \log_2 \det \left[\mathbf{I}_K + \frac{\zeta}{K}\mathbf{H}_p{}^H\mathbf{H}_p\right], \quad \text{bits/s/Hz.} \tag{5.5}$$

Note that the capacity-based AS approach, in (5.5), is based on a general formula and is not specified to a specific receiver. Moreover, this AS approach does not take into consideration the high level protocol that is running above the physical layer. However, if one attempt to maximize the throughput of the system presented in Fig.5.1, then several key parameters such as automatic-repeat-request (ARQ) techniques and DFD properties should be taking into consideration as well.

5.3.1 Performance Analysis with Perfect Channel Estimation

In this section, we assume that perfect CSI is available at the receiver while performing AS.

As mentioned in Chapter 4, if the previous decisions are correct, i.e., no propagation of

error, the different substreams can be expressed as

$$\tilde{y}_i = r_{i,i} x_i + \tilde{n}_i, \quad \text{for} \quad i = 1, 2, \ldots, K. \tag{5.6}$$

From (5.6), one can see that the resulting channel is now decomposed into K parallel virtual subchannels. Hence, the output SNR of the ith substream is given by

$$\gamma_i = r_{i,i}^2 \gamma_0, \tag{5.7}$$

where $\gamma_0 = \zeta/K$ is the average normalized received SNR at each receive antenna. Thus, the output SNRs of the substreams are determined by the diagonal entries of the matrix $\mathbf{R}$, which in turn depends on $\mathbf{E}_p$. Using (5.7) and assuming binary phase-shift keying (BPSK) transmission, the symbol error rate (SER) of the ith layer, conditioned on having correctly detected all previous symbols, is given by

$$\text{SER}_i = Q\left(\sqrt{2 r_{i,i}^2 \gamma_0}\right), \quad \text{for} \quad i = 1, 2, \ldots, K. \tag{5.8}$$

In what follows, we are interested in the probability of vector symbol error rate (V-SER), that is, the probability of at least one of the transmitted symbols in error. Hence, the conditional V-SER can be written as

$$\text{V-SER}(\mathbf{H}_p) = 1 - \prod_{i=1}^{K} (1 - \text{SER}_i). \tag{5.9}$$

From the fact that each information packet contains L/K symbols, the packet error probability (PER) can be written as

$$\text{PER}(\mathbf{H}_p) = 1 - \left[\prod_{i=1}^{K} (1 - \text{SER}_i)\right]^{L/K}. \tag{5.10}$$

Substituting (5.8) in (5.10), the PER is now given by

$$\text{PER}(\mathbf{H}_p) = 1 - \left[\prod_{i=1}^{K}\left(1 - Q\left(\sqrt{2r_{i,i}^2\gamma_0}\right)\right)\right]^{L/K}. \tag{5.11}$$

As mentioned, the selected transmit antennas are those that maximize the system throughput according to the GBN protocol [66]. Therefore, having obtained an expression for the PER as in (5.11), the throughput of the selected system can now be expressed as

$$\eta(\mathbf{H}_p) = K \cdot \frac{1 - \text{PER}(\mathbf{H}_p)}{1 + (W-1)\text{PER}(\mathbf{H}_p)}$$

$$= K \cdot \frac{\left[\prod_{i=1}^{K}\left(1 - Q\left(\sqrt{2r_{i,i}^2\gamma_0}\right)\right)\right]^{L/K}}{\left[1 + (W-1)\left(1 - \left[\prod_{i=1}^{K}\left(1 - Q\left(\sqrt{2r_{i,i}^2\gamma_0}\right)\right)\right]^{L/K}\right)\right]}, \tag{5.12}$$

where W is the window size of the GBN protocol. Note that (5.12) can be easily extended to other modulation schemes. Based on (5.12), the receiver computes the throughput for all the subsets in P', defined in (5.1). The receiver then chooses the optimal subset $p \in P'$, which has the maximum throughput value, and conveys the AS commands to the transmitter to select the optimal K antennas out of the M available ones for transmission. Keep in mind that (5.12) depends on the transmission rate, i.e., K antennas.

It is instructive now to see the behavior of (5.12) at high SNR asymptote. Thus, for SNR $\rightarrow \infty$ we have

$$\eta_\infty = \lim_{\gamma_0 \to \infty} \eta$$

$$= K. \tag{5.13}$$

Inspection of (5.13) reveals that in order to achieve the maximum throughput value M

$(K \leq M)$, the transmitter must select all the M available antennas. We stress that, even with high spatial correlation (e.g., ≥ 0.8), the transmitter is expected to select the M antennas. A possible interpretation for this is that, as the SNR approaches infinity, only the number of channel eigenmodes (eigenvalues of $H^H H$) is the more relative aspect to the system performance. It is worth noting that when we transmit a vector x through a MIMO channel, we excite the so-called eigenmodes of the channel [72]. The relative strength of these channel eigenmodes (parallel virtual subchannels), i.e., each with power gain equal to the corresponding eigenvalue, do not affect the high SNR behavior. This implies that spatial correlation has no impact on the system performance as SNR $\rightarrow \infty$.

5.3.2 Performance Analysis with Imperfect Channel Estimation

In the previous section, perfect CSI is assumed at the receiver while performing antenna selection. However, in practice, the receiver has to estimate the channel using pilot symbols. The latter are a known set of transmitted training signals. Then, the receiver uses the estimates as though it were correct to detect the transmitted packets. The effect of imperfect channel estimation on the system performance is now investigated.

In what follows, we assume that a time frame is composed of L_t pilot symbols intervals and L_d data symbols (payload) intervals. Let S denote an $M \times L_t$ training matrix, Y and Z denote the $N \times L_t$ receive and noise vectors, respectively. Thus, during training, we have

$$Y = HS + Z. \tag{5.14}$$

Following the approach in [29], one can obtain a ML estimate of H as follows:

$$
\begin{aligned}
\hat{H} &= YS^H \left(SS^H\right)^{-1} \\
&= H + ZS^H \left(SS^H\right)^{-1}.
\end{aligned}
\tag{5.15}
$$

Note that the existence of (5.15) requires the matrix SS^H to be invertible. Now, let $\Delta H = ZS^H \left(SS^H\right)^{-1}$, then

$$\hat{H} = H + \Delta H, \tag{5.16}$$

where ΔH represents the estimation error matrix of the full channel matrix H. Thus, with AS, we have

$$\hat{H}_p = H_p + \Delta H_p, \tag{5.17}$$

where ΔH_p represents the estimation error matrix corresponding to transmit antennas p. Therefore, the corresponding sampled received baseband signal can be written as

$$y = H_p \hat{E}_p x + n. \tag{5.18}$$

After having obtained the ML estimate $\hat{H}_p$, the receiver uses $\hat{H}_p$ for detection. Thus, the receiver, first performs a QR factorization of the estimated channel matrix $\hat{H}_p$ followed by nulling and cancelation. The estimated greedy QR ordered DFD can be represented by applying the QR decomposition to $\hat{H}_p$ with its columns permuted, i.e., $\hat{H}_p \hat{E}_p = \hat{Q}\hat{R}$ where $\hat{E}_p$ is a permutation matrix. Note that $\hat{E}_p$ is a function of $\hat{H}_p$. Now, the transmitted symbols are detected at the receiver as follows. Multiplying both sides of (5.18) by $\hat{Q}^H$ yields

$$
\begin{aligned}
\tilde{y} &= \hat{Q}^H \left(H_p \hat{E}_p x + n\right) \\
&= \hat{Q}^H \left[\left(\hat{H}_p - \Delta H_p\right) \hat{E}_p x + n\right] \\
&= \hat{Q}^H \left[\hat{H}_p \hat{E}_p x - \Delta H_p \hat{E}_p x + n\right] \\
&= \hat{Q}^H \hat{H}_p \hat{E}_p x - \hat{Q}^H \Delta H_p \hat{E}_p x + \tilde{n} \\
&= \hat{Q}^H \hat{Q}\hat{R} x - \hat{Q}^H \Delta H_p \hat{E}_p x + \tilde{n} \\
&= \hat{R} x - \hat{Q}^H \Delta H_p \hat{E}_p x + \tilde{n}.
\end{aligned} \tag{5.19}
$$

Let $\Omega = \hat{Q}^H \Delta H_p \hat{E}_p$ denote a $K \times K$ matrix. Then the received vector $\tilde{y}$, in matrix form,

61

can be expressed as

$$
\begin{bmatrix} \tilde{y}_1 \\ \tilde{y}_2 \\ \vdots \\ \tilde{y}_K \end{bmatrix} = \begin{bmatrix} \hat{r}_{1,1} - \Omega_{1,1} & \cdots & \hat{r}_{1,K} - \Omega_{1,K} \\ -\Omega_{2,1} & \cdots & \hat{r}_{2,K} - \Omega_{2,K} \\ \vdots & \ddots & \vdots \\ -\Omega_{K,1} & \cdots & \hat{r}_{K,K} - \Omega_{K,K} \end{bmatrix} \begin{bmatrix} x_1 \\ x_2 \\ \vdots \\ x_K \end{bmatrix} + \begin{bmatrix} \tilde{n}_1 \\ \tilde{n}_2 \\ \vdots \\ \tilde{n}_K \end{bmatrix}. \tag{5.20}
$$

Now, if we assume that all previous decisions are correct, the different substreams can be expressed as

$$
\tilde{y}_i = \hat{r}_{i,i} x_i - \sum_{j=1}^{K} \Omega_{i,j} x_j + \tilde{n}_i, \quad \text{for} \quad i = 1, 2, \ldots, K, \tag{5.21}
$$

where $\hat{r}_{i,i}$ is the (i,i)th entry of $\hat{\mathbf{R}}$. The summation term in (5.21), is analogous to effect of intersymbol interference (ISI) and can be interpreted as crosstalk among the nominally decoupled K virtual subchannels, due to estimation errors. Therefore, following a common practice in equalization analysis, we determine the post-detection SNIR. Assuming no error propagation from previous stages, the SNIR for the ith substream is given by

$$
\xi_i = \frac{\hat{r}_{i,i}^2 \lambda}{\lambda \sum_{j=1}^{K} |\Omega_{i,j}|^2 + N_0}, \tag{5.22}
$$

where $\lambda = \mathbb{E}\left[\mathbf{x}^H \mathbf{x}\right]/K$ is the average energy per symbol at the transmitter. Now, having obtained an expression for the SNIR as in (5.22), the closed-form expression for the

throughput with imperfect channel estimation can be expressed as

$$
\eta\left(\hat{\mathbf{H}}_p\right) = K \cdot \frac{1 - \mathrm{PER}\left(\hat{\mathbf{H}}_p\right)}{1 + (W-1)\mathrm{PER}\left(\hat{\mathbf{H}}_p\right)}
$$

$$
= K \cdot \frac{\left[\prod_{i=1}^{K}\left(1 - Q\left(\sqrt{\dfrac{2\hat{r}_{i,i}^2\lambda}{\lambda\sum_{j=1}^{K}\left|\Omega_{i,j}\right|^2 + N_0}}\right)\right)\right]^{L/K}}{\left[1 + (W-1)\left(1 - \left[\prod_{i=1}^{K}\left(1 - Q\left(\sqrt{\dfrac{2\hat{r}_{i,i}^2\lambda}{\lambda\sum_{j=1}^{K}\left|\Omega_{i,j}\right|^2 + N_0}}\right)\right)\right]^{L/K}\right)\right]} .
$$

(5.23)

5.4 Simulation Results

Simulation results are now presented for the cross-layer AS approach in correlated flat Ricean fading MIMO channels. Performance results are reported in terms of the throughput versus E_s/N_0 in dB. Note that the link layer throughput is measured as the effective number of correctly received bits at the link layer per channel use [66]. In the following, a system with M transmit and N receive antenna is referred as an $M \times N$ system. Henceforth, we consider: *i*) 4×4 MIMO system; *ii*) GBN window with $W = 4$ packets; *iii*) frame duration of 2 ms; *iv*) frame length is $L = 180$ symbols; *v*) Ricean factor is set to $\kappa = 3$ dB; *vi*) exponential correlation model.

5.4.1 Perfect Channel Estimation

Fig. 5.2 shows the system performance with both cross-layer and capacity-based AS approaches. We consider two correlation settings: *i*) $|\rho| = 0$ (uncorrelated case); *ii*) $|\rho| = 0.6$. We plot along an additional curve, as a benchmark, for the same system without performing AS. It can be noticed that the performance of the cross-layer AS is significantly better than the capacity-based one. In fact, it can be seen that the throughput gain is large at moderate

SNRs. Inspection of Fig. 5.2 reveals that the cross-layer AS is more robust to the effect of spatial correlation at low SNRs ($[0-7]$ dB). Note that the performance degradation is about 2 dB for the cross-layer AS, whereas it is about 3 dB for the capacity-based one.
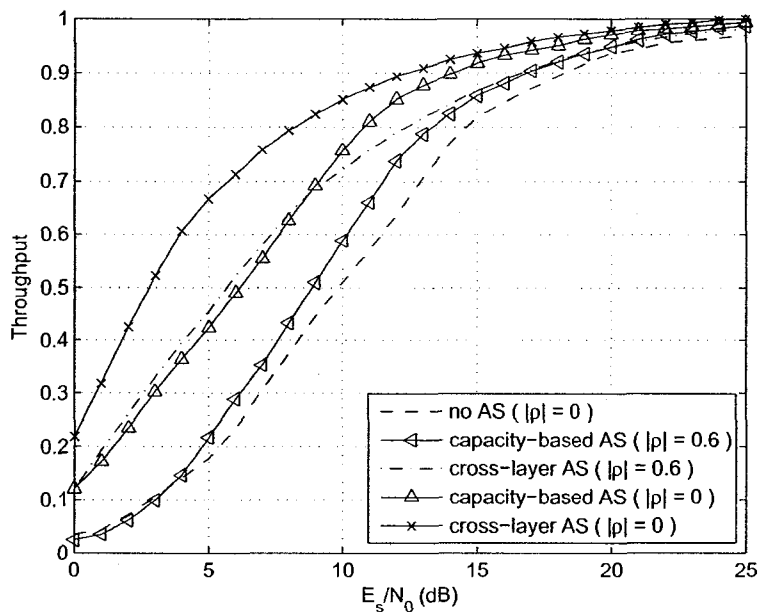

Figure 5.2: Normalized throughput performance of a 4×4 system performing both cross-layer and optimal capacity-based AS. $\kappa = 3$ dB, exponential correlation model, BPSK constellations.

Fig. 5.3 depicts the effects of spatial correlation on the cross-layer AS approach for the 4×4 MIMO system. We consider five correlation settings: i) $|\rho| = 0$ (uncorrelated case); ii) $|\rho| = 0.4$; iii) $|\rho| = 0.6$; iv) $|\rho| = 0.8$; v) $|\rho| = 0.9$. Conclusions that can be drawn, by examining Fig. 5.3, is that spatial correlation reduces the effective SNRs of the data substreams and hence lead to a degradation in the performance.

Fig. 5.4 shows the average SNR loss due to spatial correlation for the 4×4 MIMO system performing cross-layer AS. Note that the average SNR loss, for a predefined throughput
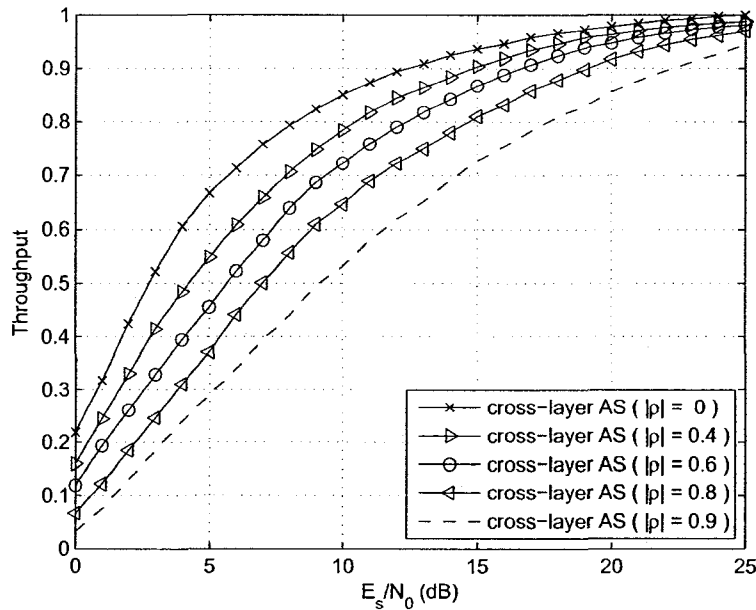
Figure 5.3: Normalized throughput of a 4×4 system performing cross-layer AS under different exponential correlation settings. $\kappa = 3$ dB, BPSK constellations.

η and correlation values $|\rho|$, is defined by

$$\text{loss(dB)} = \text{SNR}(|\rho| = x) - \text{SNR}(|\rho| = 0). \tag{5.24}$$

For instance, the average SNR loss for $\eta = 0.5$ with $|\rho| = 0.4$ is about 1 dB. It can be seen that the average SNR loss increases with the correlation coefficients $|\rho|$, and the loss rate reaches 3 dB when $|\rho|$ increases up to 0.7. Note that the average SNR loss increases steeply when correlation exceeds $|\rho| = 0.8$.

In Fig. 5.5, the usage rate of each antenna combination of the cross-layer AS approach is shown. In these results, we consider the same correlation settings as in Fig. 5.3. An inspection of Fig. 5.5 discloses qualitatively different behaviors at moderate SNRs (e.g., $[0 - 12]$ dB). More precisely, the rate of usage of each antenna combination with high spatial correlation of $|\rho| = 0.8, 0.9$ (this corresponds to a severe lack of angular spread
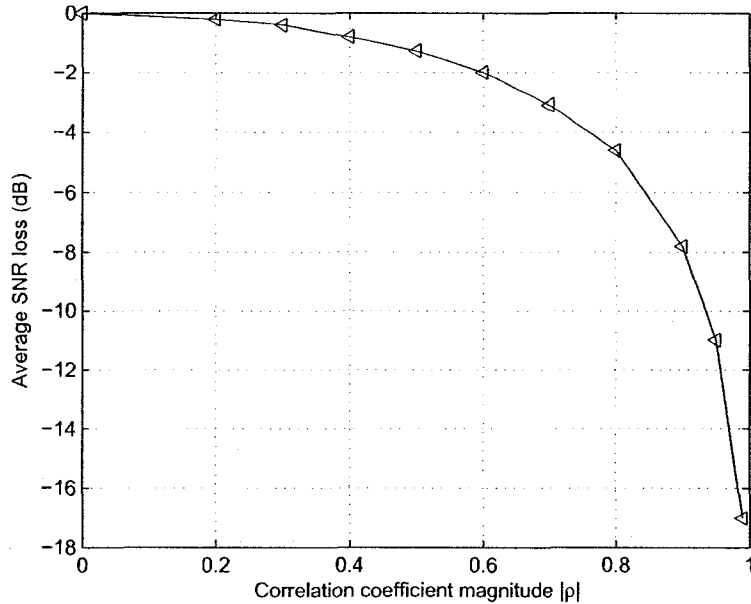
Figure 5.4: Average SNR loss due to spatial correlation for a 4×4 system employing cross-layer AS. $\kappa = 3\,dB$, exponential correlation model, BPSK constellations.

or closely spaced antennas) [45] reveals different behavior than that with moderate spatial correlation of $|\rho| = 0, 0.4, 0.6$. For instance, at high spatial correlation, the one antenna combination is the dominant one where it reaches approximately 100% with $|\rho| = 0.9$. A primary reason for the difference can be explained intuitively as follows. At high spatial correlation and at moderate SNRs, the cross-layer AS tends to choose the minimum number of antennas in an attempt to reduce the effect of spatial correlation as possible (e.g., $|\rho| = 0.8, 0.9$). In other words, under these conditions, it is better to transmit less information with higher reliability. At high SNRs (e.g., $\geq 16\,dB$), the usage rate behavior is slightly affected by spatial correlation where the four antenna combination is the most employed. It is worth noting that this observation conforms with $\eta_\infty = K$ given in (5.13). Thus in order to achieve the maximum throughput value M ($K \leq M$), the transmitter must select all the M available antennas. In other words, as the SNR approaches infinity, only
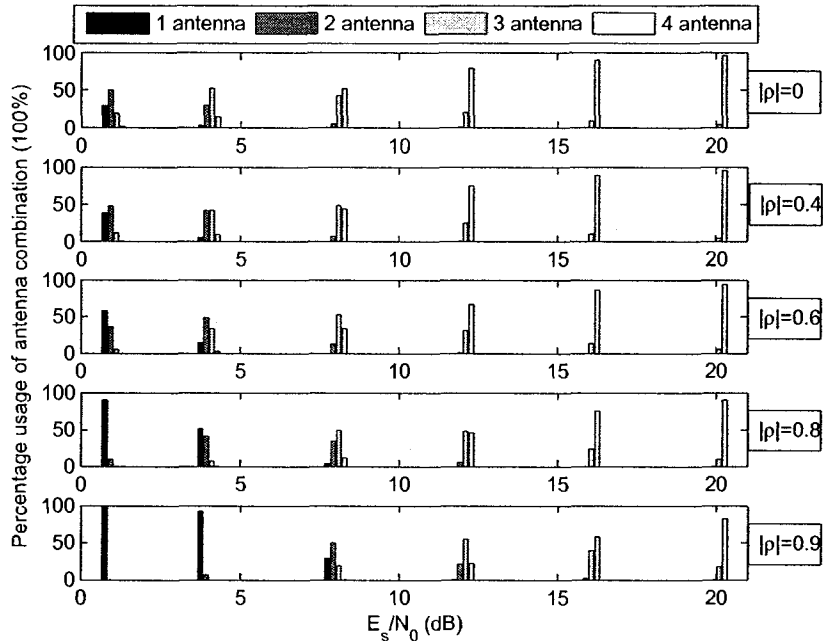
Figure 5.5: Usage rate of transmit antenna combination, active antenna K, of a 4×4 system performing cross-layer AS. $\kappa = 3$ dB, exponential correlation model, BPSK constellations.

the number of channel eigenmodes (eigenvalues of $\mathbf{H}^H\mathbf{H}$) is the more relative aspect to the system performance. It is worth noting that when we transmit a vector $\mathbf{x}$ through a MIMO channel, we excite the so-called eigenmodes of the channel [72]. The relative strength of these channel eigenmodes (parallel virtual subchannels), i.e., each with power gain equal to the corresponding eigenvalue, do not affect the high SNR behavior. Therefore, at high SNRs, the effective impact of spatial correlation decreases.

The rate of usage of each antenna combination using the capacity-based AS is depicted in Fig. 5.6. For a fair comparison, we use the same correlation settings as in Fig. 5.5. One can directly notice that, at low/high SNR, the capacity-based AS exhibits approximately the same usage rate behavior with four antenna combination being dominant. It follows that the usage rate of each antenna combination, for the capacity-based AS, is slightly affected by spatial correlation. It can be seen that the existence of spatial correlation ($|\rho| > 0$)
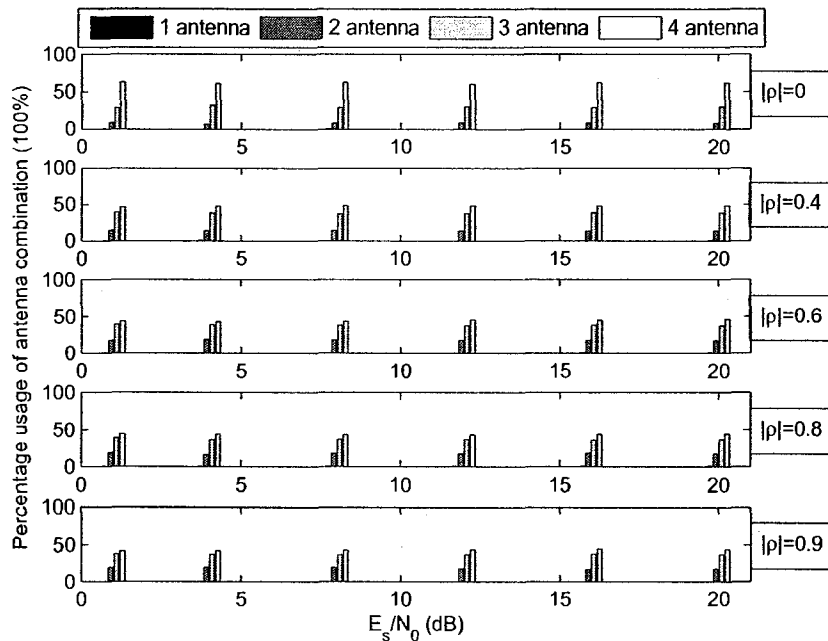
67

Figure 5.6: Usage rate of transmit antenna combination, active antenna K, of a 4×4 system performing capacity-based AS. $\kappa = 3$ dB, exponential correlation model, BPSK constellations.

slightly decreases the usage rate of the four antenna combination at moderate SNRs. This ties well with intuition since the presence of spatial correlation can raise the possibility of moderately to severely ill-conditioned channel matrix, i.e., rank-deficient channel matrix $\mathbf{H}$ ($\text{rank}(\mathbf{H}) < \min(N,M)$) [45]. Now, keep in mind the fact that the optimal choice of K transmit antennas that maximizes the channel capacity results in a channel matrix that is full rank ($\text{rank}(\mathbf{H}_p) = K$) [23]. Thus, this explains the decrease in the usage rate of the four antenna combination. Note that in the limit $|\rho| \to 1$, we have a rank-one/keyhole channel matrix $\mathbf{H}$ (this corresponds to the case when signals have to go through windows in buildings). Therefore, the best strategy is to select only the antenna with the highest channel gain . To summarize, contrary to the cross-layer AS, the capacity-based AS always tends to select the maximum number of antenna combination to achieve the maximum possible physical data rate.

5.4.2 Imperfect Channel Estimation

In this section, we investigate the impact of imperfect channel estimation on the cross-layer AS. To isolate the effects of imperfect channel estimation from that of spatial correlation, we consider independent Ricean flat fading channels (i.e., $|\rho| = 0$). We stress that in simulation, training symbols are not counted in the throughput computation.

Fig. 5.7 depicts the system throughput performance with the cross-layer AS. We consider four training-sequence lengths: $i)$ $L_t = 4$ symbols; $ii)$ $L_t = 10$ symbols; $iii)$ $L_t = 20$ symbols; $iv)$ $L_t = 100$ symbols. We plot an additional curve, as a benchmark, for the case where the receiver perfectly estimates the channel. It is clear that with a training-sequence of length $L_t = 100$ the performance is very close to that of perfect CSI. Thus a longer training-sequence yields a higher throughput. Decreasing the training-sequence length, from $L_t = 100$ to $L_t = 20$ symbols, increases the SNR loss to about 3 dB. Also the SNR penalty, due to imperfect channel estimation, is about 5 dB and 15 dB with $L_t = 10$ and 4 symbols, respectively. Note that with $L_t = 4$ symbols, the system performs poorly with an asymptotic error floor where the throughput reaches a maximum 0.6 regardless of the SNR. This follows from the fact that a short training-sequence length, $L_t = 4$, is insufficient to capture the dynamics of the rapidly fading channel. Therefore, imperfect channel estimates lead to propagation of errors in the subsequent nulling and cancelation stages in the DFD, and also affect the greedy QR detection ordering, which in turn limits the performance of the DFD.

The impact of imperfect channel estimation on the system performance with capacity-based AS, for various training-sequence lengths, is displayed in Fig. 5.8. It can be observed that, the capacity-based AS with $L_t = 100$ symbols exhibits a very close performance to that with perfect CSI. For instance, for $\eta = 0.4$ with $L_t = 100$ symbols, SNR penalty of 0.5 dB is incurred. Decreasing the training-sequence length to $L_t = 20, 10, 4$ symbols increases the SNR loss to approximately 2 dB, 3 dB, and 15 dB respectively. Similar to the cross-layer
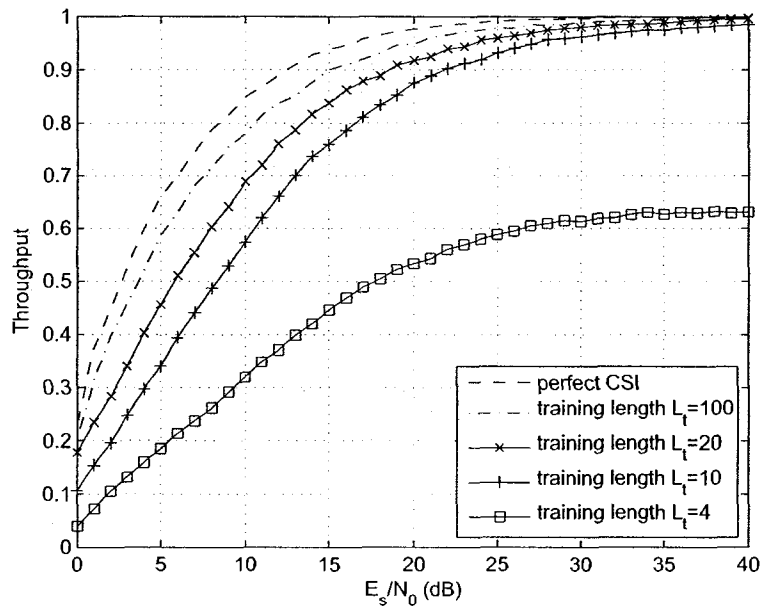
Figure 5.7: The impact of imperfect channel estimation on the performance of a 4×4 system performing cross-layer AS. $\kappa = 3\ dB$, uncorrelated case $(|\rho| = 0)$, BPSK constellations.
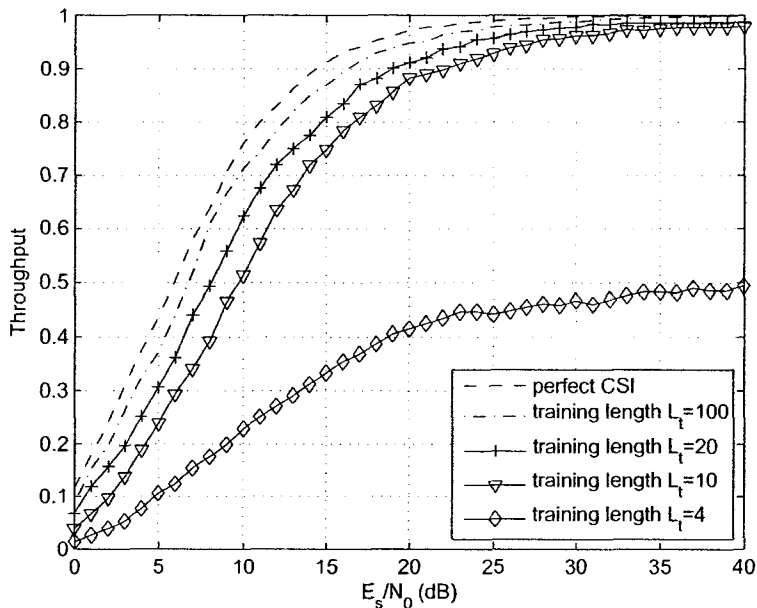
Figure 5.8: The impact of imperfect channel estimation on the performance of a 4×4 system performing capacity-based AS. $\kappa = 3\ dB$, uncorrelated case ($|\rho| = 0$), BPSK constellations.

AS with $L_t = 4$, the performance is limited by an error floor caused by channel estimation errors where the throughput reaches a maximum of 0.5.

Comparison of the throughput performance for the 4×4 MIMO system, with training-sequence length $L_t = 10$, performing cross-layer and capacity-based AS is displayed in Fig. 5.9. For a meaningful comparison, we plot along curves for cross-layer and capacity-based AS, with perfect CSI at the receiver. Examining Fig. 5.9 reveals that capacity-based AS is more tolerant/robust to imperfect channel estimation. For instance, for $\eta = 0.5$, the SNR penalty loss is about 5 dB and 3 dB for cross-layer and capacity-based AS, respectively.

The rate of usage of each antenna combination using the cross-layer AS and under imperfect channel estimation, is depicted in Fig. 5.10. Note that the rate of usage with $L_t = 100, 20, 10$, exhibits a similar behavior to that with perfect CSI, whereas for $L_t = 4$
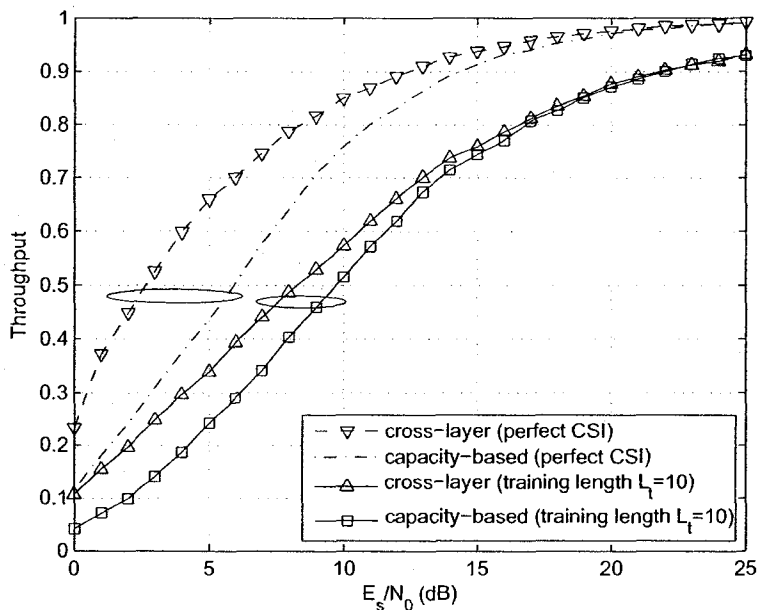
Figure 5.9: Comparison of the impact of imperfect channel estimation on a 4×4 system employing both cross-layer and capacity-based AS, with training-sequence length $L_t = 10$. $\kappa = 3 \, dB$, uncorrelated case ($|\rho| = 0$), BPSK constellations.

symbols, the three antenna combination is the most employed over the range of SNRs.

Finally, the usage rate of each antenna combination using the capacity-based AS and under imperfect channel estimation is displayed in Fig 5.11. In contrast to the cross-layer AS usage rate behavior, the capacity-based AS usage rate is independent of the reliability of the channel estimates obtained using different training-sequence lengths and somehow similar to that with perfect CSI. Note that the four antenna combination is again the most adopted in this approach over all SNRs. Thus, unlike the cross-layer AS approach, the antenna usage rate of the capacity-based AS is less affected by the nonideal channel conditions (spatial correlation and imperfect channel estimation). However, in all cases, the cross-layer AS approach is still able to achieve a better throughput performance than the capacity-based AS.

Figure 5.10: Usage rate of transmit antenna combination, active antenna K, of a 4×4 system performing cross-layer AS with various training-sequence length settings. $\kappa = 3\,dB$, uncorrelated case ($|\rho| = 0$), BPSK constellations.
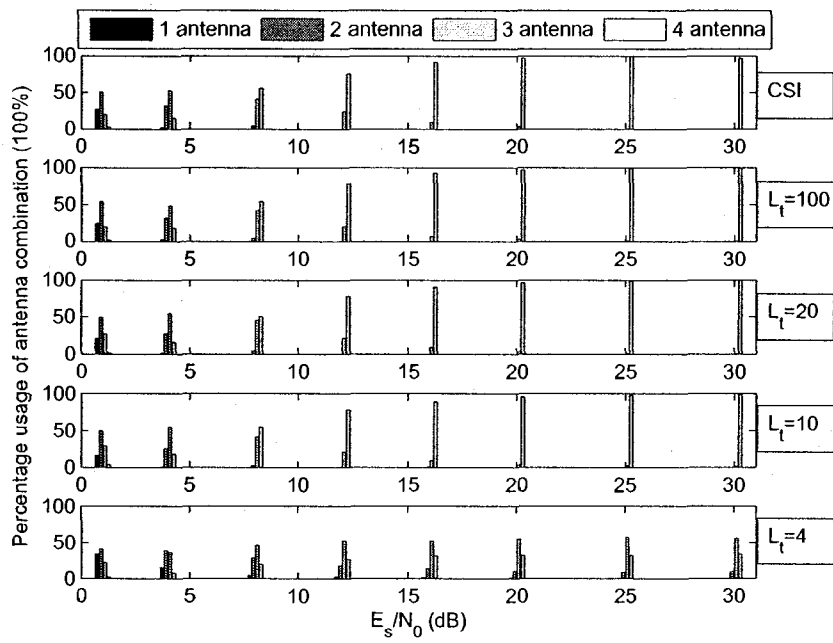
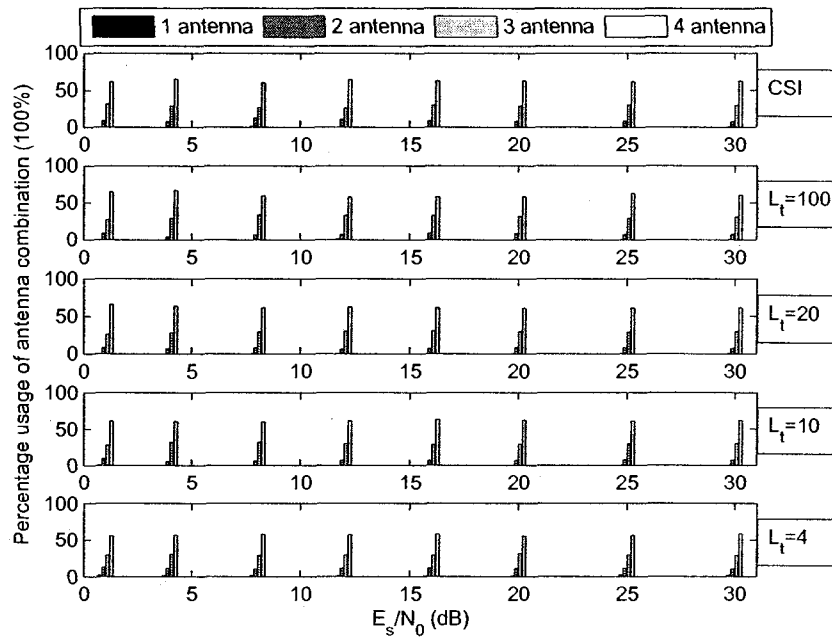Figure 5.11: Usage rate of transmit antenna combination, active antenna K, of a 4×4 system performing capacity-based AS with various training-sequence length settings. $\kappa = 3$ dB, uncorrelated case ($|\rho| = 0$), BPSK constellations.

5.5 Conclusions

We investigated the performance of a cross-layer AS approach for the DFD in MIMO systems. We have assumed a spatially correlated flat Ricean fading MIMO model, which is known more accurately to model real-world wireless environments. A closed-form expression for the system throughput with perfect channel estimation was derived. We further analyzed the system performance with pilot-aided channel estimation. In that, we derived a closed-form expression for the post-detection SNIR of each substream. Furthermore, we have shown that the cross-layer AS always assigns transmissions to the antenna combination which sees the better channel conditions, resulting in a substantial improvement over the optimal capacity-based AS. It has been shown that the latter is more robust to nonideal channel conditions such as spatial correlation and imperfect channel estimation. However, in all cases, the cross-layer AS approach is able to outperform the capacity-based AS.

Chapter 6

Conclusions and Future Work

This chapter summarizes the major contributions in this thesis and presents possible future directions which could be extensions of the research work in this thesis.

6.1 Conclusions

- Chapter 3 analyzed the probability of bit error of the ZF receiver in transmit correlated Ricean flat-fading channels. Specifically, we have derived a near exact approximation for the average BER of each substream with QPSK modulation. Furthermore, we have derived a closed-form expression for the optimal transmit correlation coefficient which achieves the maximum capacity (i.e., uncorrelated case) of TITO-SM systems. Simulation results have showed the accuracy of the given analysis. Also we have observed that, in receive correlated Ricean flat-fading channels, the system performance when $N = M$ is the same as that of transmit correlated Ricean flat-fading channels.

- In chapter 4, we have analyzed the performance of an AS approach for the DFD receiver over independent Rayleigh flat-fading channels. We used a pragmatic selection criterion that maximizes both the post-processing SNR at the receiver end, and

the system capacity. We have derived an upper bound expression on the outage probability for the AS at high-SNR regime. We have also shown that the performance of the proposed AS scheme is comparable to the optimal selection based on exhaustive search, but with much less complexity.

- In Chapter 5, we have presented a cross-layer AS approach for the DFD in MIMO systems. A spatially correlated Ricean flat-fading MIMO model was assumed. A closed-form expression for the system throughput with perfect channel estimation was derived. Further the system performance with pilot-aided channel estimation is analyzed. In that, we derived a closed-form expression for the post-detection SNIR of each substream. In addition, we have shown that the cross-layer AS always assigns transmissions to the antenna combination which sees the better channel conditions, resulting in a substantial improvement over the optimal capacity-based AS. It has been shown that the latter is more robust to nonideal channel conditions such as spatial correlation and imperfect channel estimation. However, in all cases, the cross-layer AS approach is able to outperform the capacity-based AS.

6.2   Future Directions

Although this thesis has investigated the BER performance of ZF receivers, and proposed AS approaches for the DFD, there are several issues that remain to be explored. In this section, we discuss several important areas which require further study.

- An important point that is not addressed in this thesis is the effect of delay and errors in the feedback channel in Chapters 4 and 5. This will affect the optimal choice of the selected antennas and lead to a degradation of the system performance compared with ideal channels. A detailed analysis, along the lines of [74] is a possible avenue of future work.

- The analysis provided, in chapter 3, was only for independent Rayleigh matrix channels, which are known to be ideal in practice. Analysis in different environments such as correlated Ricean fading channels is an interesting topic for future research.

- In Chapters 3 and 4, performance analyses were provided under the assumption of perfect CSI at the receiver. However, in reality the receiver has to resort to an estimate of $\mathbf{H}$. This will lead to a degradation of performance compared with ideal channels. Therefore performance analyses under imperfect channel estimation are important issues for future research.

- The Kronecker correlation model, adopted in Chapters 3 and 5 neglects the statistical interdependence of both link ends. Recently, a stochastic model for modeling spatial correlation in MIMO radio channels has been proposed in [75]. This model takes into account the joint correlation properties of both link ends. Therefore, performance analyses in this case are possible for future avenue.

- Performance analyses of the proposed AS schemes under the so-called *keyhole* or *pinhole* [43] channel model are also important issues for future research.

Bibliography

[1] J. H. Winters, "On the capacity of radio communication systems with diversity in a Rayleigh fading environment," *IEEE J. Sel. Areas Commun.*, vol. 5, pp. 871–878, Jun. 1987.

[2] G. J. Foschini and M. J. Gans, "On limits of wireless communications in a fading environment when using multiple antennas," *Wireless Personal Communications*, vol. 6, pp. 311–335, Nov. 1998.

[3] I. E. Telatar, "Capacity of multi-antenna Gaussian channels," *European Transactions on Telecommunications*, vol. 10, pp. 585–595, Nov./Dec. 1999.

[4] G. J. Foschini, "Layered space-time architecture for wireless communication in a fading environment when using multi-element antennas," *Bell Labs Technical Journal*, vol. 1, pp. 41–59, Autumn 1996.

[5] J. G. Proakis, *Digital Communications*. New York: 4th ed. McGraw-Hill Press, 2001.

[6] A. J. Paulraj, D. A. Gore, R. U. Nabar, and H. Bolcskei, "An overview of MIMO communications-a key to gigabit wireless," *Proc. IEEE*, vol. 92, pp. 198–218, Feb. 2004.

[7] S. M. Alamouti, "A simple transmit diversity technique for wireless communications," *IEEE J. Sel. Areas Commun.*, vol. 16, pp. 1451–1458, Oct. 1998.

[8] V. Tarokh, N. Seshadri, and A. R. Calderbank, "Space-time codes for high data rate wireless communication: performance criterion and code construction," *IEEE Trans. Inf. Theory*, vol. 44, pp. 744–765, Mar. 1998.

[9] V. Tarokh, H. Jafarkhani, and A. R. Calderbank, "Space-time block codes from orthogonal designs," *IEEE Trans. Inf. Theory*, vol. 45, pp. 1456–1467, Jul. 1999.

[10] L. Zheng and D. N. C. Tse, "Diversity and multiplexing: a fundamental tradeoff in multiple-antenna channels," *IEEE Trans. Inf. Theory*, vol. 49, pp. 1073–1096, May 2003.

[11] R. W. Health and D. J. Love, "Multimode antenna selection for spatial multiplexing systems with linear receivers," *IEEE Trans. Signal Process.*, vol. 53, pp. 3042–3056, Aug. 2005.

[12] D. Gore, R. W. Health, and A. Paulraj, "On performance of the zero forcing receiver in presence of transmit correlation," in *Proc. IEEE International Symposium on Information Theory (ISIT02)*, Lausanne, Switzerland, Jun./Jul. 2002, p. 159.

[13] Z. Xu and R. D. Murch, "Performance analysis of maximum likelihood detection in a MIMO antenna system," *IEEE Trans. Commun.*, vol. 50, pp. 187–191, Feb. 2002.

[14] M. K. Varanasi and T. Guess, "Optimum decision feedback multiuser equalization with successive decoding achieves the total capacity of the Gaussian multiple-access channel," in *Proc. Thirty-First Asilomar Conference on Signals, Systems and Computers*, Pacific Grove, California, Nov. 1997, pp. 1405–1409.

[15] P. W. Wolniansky, G. J. Foschini, G. D. Golden, and R. A. Valenzuela, "V-BLAST: an architecture for realizing very high data rates overthe rich-scattering wireless channel," in *Proc. URSI International Symposium on Signals, Systems, and Electronics (ISSSE98)*, Pisa, Italy, Sep. 1998, pp. 295–300.

[16] G. J. Foschini, G. D. Golden, R. A. Valenzuela, and P. W. Wolniansky, "Simplified processing for high spectral efficiency wireless communication employing multi-element arrays," *IEEE J. Sel. Areas Commun.*, vol. 17, pp. 1841–1852, Nov. 1999.

[17] G. D. Golden, G. J. Foschini, R. A. Valenzuela, and P. W. Wolniansky, "Detection algorithm and initial laboratory results using V-BLAST space-time communication architecture," *Electron. Lett.*, vol. 92, pp. 14–16, Jan. 1999.

[18] A. F. Molisch and M. Z. Win, "MIMO systems with antenna selection," *IEEE Microw. Mag.*, vol. 5, pp. 46–56, Mar. 2004.

[19] S. Sanayei and A. Nosratinia, "Antenna selection in MIMO systems," *IEEE Commun. Mag.*, vol. 42, pp. 68–73, Oct. 2004.

[20] D. Shiu, G. J. Foschini, and J. M. Khan, "Fading correlation and its effect on the capacity of multi-element antenna systems," *IEEE Trans. Commun.*, vol. 48, pp. 502–513, Mar. 2000.

[21] R. Xu and F. C. M. Lau, "Performance analysis for MIMO systems using zero forcing detector over Rice fading channel," in *Proc. IEEE International Symposium on Circuits and Systems (ISCAS05)*, Kobe, Japan, May 2005, pp. 4955–4958.

[22] G. L. Stuber, *Principles of Mobile Communications*. Kluwer: Norwell, MA, 1996.

[23] D. A. Gore, R. U. Nabar, and A. Paulraj, "Selecting an optimal set of transmit antennas for a low rank matrix channel," in *Proc. IEEE International Acoustics, Speech, and Signal Processing (ICASSP00)*, Istanbul, Turkey, Jun. 2000, pp. 2785–2788.

[24] A. Gorokhov, D. A. Gore, and A. J. Paulraj, "Receive antenna selection for MIMO spatial multiplexing: theory and algorithms," *IEEE Trans. Signal Process.*, vol. 51, pp. 2796–2807, Nov. 2003.

[25] R. W. Health, S. Sandhu, and A. Paulraj, "Antenna selection for spatial multiplexing systems with linear receivers," *IEEE Commun. Lett.*, vol. 5, pp. 142–144, Apr. 2001.

[26] J. L. Vicario, M. A. Lagunas, and C. Anton-Haro, "A cross-layer approach to transmit antenna selection," *IEEE Trans. Wireless Commun.*, vol. 5, pp. 1993–1997, Aug. 2006.

[27] J. P. Kermoal, L. Schumacher, K. Ingemann, P. E. Mogensen, and F. Frederiksen, "A stochastic MIMO radio channel model with experimental validation," *IEEE J. Sel. Areas Commun.*, vol. 20, pp. 1211–1226, Aug. 2002.

[28] S. K. Jayaweera and H. V. Poor, "On the capacity of multiple-antenna systems in Rician fading," *IEEE Trans. Wireless Commun.*, vol. 4, pp. 1102–1111, May 2005.

[29] T. L. Marzetta, "BLAST training: estimating channel characteristics for high capacity space-time wireless," in *Proc. 37th Annual Allerton Conference on Communication, Control, and Computing*, Monticello, IL, Sep. 1999, pp. 958–966.

[30] B. Hassibi, "A fast square-root implementation for BLAST," in *Proc. Thirty-Fourth Asilomar Conference on Signals, Systems and Computers*, Pacific Grove, CA, USA, Sep. 2000, pp. 1255–1259.

[31] M. Sellathurai and S. Haykin, "Turbo-BLAST for wireless communications: theory and experiments," *IEEE Trans. Signal Process.*, vol. 50, pp. 2538–2546, Oct. 2002.

[32] J. Benesty, Y. Huang, and J. Chen, "A fast recursive algorithm for optimum sequential signal detection in a BLAST system," *IEEE Trans. Signal Process.*, vol. 51, pp. 1722–1730, Jul. 2003.

[33] E. Viterbo and J. Buotros, "A universal lattice code decoder for fading channels," *IEEE Trans. Inf. Theory*, vol. 45, pp. 1639–1642, Jul. 1999.

[34] J. H. Winters, J. Salz, and R. D. Gitlin, "The impact of antenna diversity on the capacity of wireless communication systems," *IEEE Trans. Commun.*, vol. 42, pp. 1740–1751, Feb. 1994.

[35] A. J. Viterbi, "Very low rate convolutional codes for maximum theoretical performance of spread-spectrum multiple-access channels," *IEEE J. Sel. Areas Commun.*, vol. 8, pp. 641–649, May 1990.

[36] P. Patel and J. Holtzman, "Analysis of a simple successive interference cancellation scheme in a DS/CDMA system," *IEEE J. Sel. Areas Commun.*, vol. 12, pp. 796–807, Jun. 1994.

[37] S. Loyka and F. Gagon, "Performance analysis of the V-BLAST algorithm: an analytical approach," *IEEE Trans. Wireless Commun.*, vol. 3, pp. 1326–1337, Jul. 2004.

[38] Y. Jiang, X. Zheng, and J. Li, "Asymptotic performance analysis of V-BLAST," in *Proc. IEEE Global Telecommunications Conference (GLOBECOM05)*, Saint Louis, MO, Nov. 2005, pp. 3882–3886.

[39] S. Loyka, "V-BLAST outage probability: analytical analysis," in *Proc. IEEE Vehicular Technology Conference (VTC02)*, Vancouver, Canada, Sep. 2002, pp. 1997–2001.

[40] C. Shen, Y. Zhu, S. Zhou, and J. Jiang, "On the performance of V-BLAST with zero-forcing successive interference cancellation receiver," in *Proc. IEEE Global Telecommunications Conference (GLOBECOM04)*, Texas, USA, Nov. 2004, pp. 2818–2822.

[41] S. Loyka and F. Gagon, "V-BLAST without optimal ordering: analytical performance evaluation for Rayleigh fading channels," *IEEE Trans. Commun.*, vol. 54, pp. 1109–1120, Jun. 2006.

[42] S. Loyka and F. Gagnon, "Analytical BER analysis of the V-BLAST in a Rayleigh fading channel," in *Proc. IEEE Wireless Communications and Networking Conference (WCNC06)*, Las Vegas, USA, Apr. 2006, pp. 827–832.

[43] D. Chizhik, G. J. Foschini, M. J. Gans, and R. A. Valenzuela, "Keyholes, correlations, and capacities of multielement transmit and receive antennas," *IEEE Trans. Wireless Commun.*, vol. 1, pp. 361–368, Apr. 2002.

[44] O. Fernandez, M. Domingo, and R. P. Torres, "Empirical analysis of the correlation of MIMO channels in indoor scenarios at 2 GHz," *IEE Proc. Commun.*, vol. 152, pp. 82–88, Feb. 2005.

[45] D. Gesbert, H. Bolcskei, D. A. Gore, and A. J. Paulraj, "Outdoor MIMO wireless channels: models and performance prediction," *IEEE Trans. Commun.*, vol. 50, pp. 1926–1934, Dec. 2002.

[46] C. N. Chuah, D. N. C. Tse, J. M. Kahn, and R. A. Valenzuela, "Capacity scaling in MIMO wireless systems under correlated fading," *IEEE Trans. Inf. Theory*, vol. 48, pp. 637–650, Mar. 2002.

[47] L. Yang and J. Qin, "Performance of STBCs with antenna selection: spatial correlation and keyhole effects," *IEE Proc. Commun.*, vol. 153, pp. 15–20, Feb. 2006.

[48] T. Ratnarajah, "Spatially correlated multiple-antenna channel capacity distributions," *IEE Proc. Commun.*, vol. 153, pp. 263–271, Apr. 2006.

[49] S. Loyka, "Channel capacity of MIMO architecture using the exponential correlation matrix," *IEEE Commun. Lett.*, vol. 5, pp. 369–371, Sep. 2001.

[50] R. Narasimhan, "Finite-SNR diversity-multiplexing tradeoff for correlated Rayleigh and Ricean MIMO channels," *IEEE Trans. Inf. Theory*, vol. 52, pp. 3965–3979, Sep. 2006.

[51] H. Bölcskei, *Principles of MIMO-OFDM wireless systems.* Florida, USA: CRC Press, 2004.

[52] M. A. Khalighi, J. M. Brossier, G. Jourdain, and K. Raoof, "On capacity of Ricean MIMO channels," in *Proc. IEEE International Symposium On Personal Indoor and Mobile Communications (PIMRC01)*, San Diego, USA, Sep. 2001, pp. 150–154.

[53] R. J. Muirhead, *Aspects of Multivariate Statistical Theory.* Hoboken, New Jersey: Wiley series in probability and statistics, 2005.

[54] W. Y. Tan and R. P. Gupta, "On approximating the non-central Wishart distribution with Wishart distribution," *Communication in Statistical Theory and Method*, vol. 12, pp. 2589–2600, 1983.

[55] T. Eng and L. B. Milstein, "Coherent DS-CDMA performance in Nakagami multipath fading," *IEEE Trans. Commun.*, vol. 43, pp. 1134–1143, Feb./Mar./Apr. 1995.

[56] H. A. A. Saleh and W. Hamouda, "Performance of zero-forcing detectors over MIMO flat correlated Ricean fading channels," *IET Commun.*, accepted for publication (to appear).

[57] R. W. Health and A. Paulraj, "Antenna selection for spatial multiplexing systems based on minimum error rate," in *Proc. IEEE International Conference on Communications (ICC01)*, Helsinki, Finland, Jun. 2001, pp. 2276–2280.

[58] A. F. Molisch, M. Z. Win, and J. H. Winters, "Capacity of MIMO systems with antenna selection," in *Proc. IEEE International Conference on Communications (ICC01)*, Helsinki, Finland, Jun. 2001, pp. 570–574.

[59] D. A. Gore, R. W. Health, and A. J. Paulraj, "Transmit selection in spatial multiplexing systems," *IEEE Commun. Lett.*, vol. 6, pp. 491–493, Nov. 2002.

[60] A. Gorokhov, "Antenna selection algorithms for MEA transmission systems," in *Proc. IEEE International Acoustics, Speech, and Signal Processing (ICASSP02)*, Orlando, Florida, May 2002, pp. 2857–2860.

[61] D. Wubben, R. Bohnke, J. Rinas, V. Kuhn, and K. D. Kammeyer, "Efficient algorithm for decoding layered space-time codes," *IEE Electron. Lett.*, vol. 37, pp. 1348–1350, Oct. 2001.

[62] H. A. David, *Order Statistics*, 2nd ed. New York: Wiley-Interscience, 1970.

[63] A. M. Tulino and S. Verdú, *Random Matrix Theory and Wireless Communications.* Hanover, MA 02339 USA:: now Publishers Inc., 2004.

[64] M. Abramowitz and I. A. Stegun, *Handbook of Mathematical Functions: With Formulas, Graphs, and Mathematical Tables*. Mineola, NY: Dover Press, 1964.

[65] H. A. A. Saleh and W. Hamouda, "Antenna selection approach for decision-feedback detectors over MIMO flat fading channels," in *Proc. 24th Biennial Symposium on Communications (BSC08)*, Kingston, Ontario, Jun. 2008, pp. 270–273.

[66] S. Lin, D. Costello, and M. Miller, "Automatic-repeat-request error-control schemes," *IEEE Commun. Mag.*, vol. 22, pp. 5–17, Dec. 1984.

[67] Y. Jiang and M. K. Varanasi, "The effect of ordered detection and antenna selection on diversity gain of decision feedback detector," in *Proc. IEEE International Conference on Communications (ICC07)*, Glasgow, Scotland, Jun. 2007, pp. 5383–5388.

[68] D. Chizhik, F. Rashid-Farrokhi, J. Ling, and A. Lozano, "Effect of antenna separation on the capacity of BLAST in correlated channels," *IEEE Commun. Lett.*, vol. 4, pp. 337–339, Nov. 2000.

[69] A. Hjørungnes and D. Gesbert, "Precoded orthogonal space-time block codes over correlated Ricean MIMO channels," *IEEE Trans. Signal Process.*, vol. 55, pp. 779–783, Feb. 2007.

[70] A. Paulraj, R. Nabar, and D. Gore, *Introduction to Space-Time Wireless Communications*. Cambridge, U.K.: Cambridge Univ. Press, 2003.

[71] C. Martin and B. Ottersten, "Asymptotic eigenvalue distributions and capacity for MIMO channels under correlated fading," *IEEE Trans. Wireless Commun.*, vol. 3, pp. 1350–1359, Jul. 2004.

[72] S. Barbarossa, *Multiantenna Wireless Communication Systems*. Norwood, USA: Artech House, 2005.

[73] S. Sanayei and A. Nosratinia, "Antenna selection in keyhole channels," *IEEE Trans. Commun.*, vol. 55, pp. 404–408, Mar. 2007.

[74] E. N. Onggosanusi, A. Gatherer, A. G. Dabak, and S. Hosur, "Performance analysis of closed-loop transmit diversity in the presence of feedback delay," *IEEE Trans. Commun.*, vol. 49, pp. 1618–1630, Sep. 2001.

[75] W. Weichselberger, M. Herdin, H. Ozcelik, and E. Bonek, "A stochastic MIMO channel model with joint correlation of both link ends," *IEEE Trans. Wireless Commun.*, vol. 5, pp. 90–100, Jan. 2006.